Genome analyses show strong selection on coloration, morphological and behavioral phenotypes in birds-of-paradise.

Stefan Prost[1,2,*], Ellie E. Armstrong[1], Johan Nylander[3], Gregg W.C. Thomas[4], Alexander Suh[5], Bent Petersen[6,7], Love Dalen[3], Brett W. Benz[8], Mozes P.K. Blom[3], Eleftheria Palkopoulou[3], Per G. P. Ericson[3], Martin Irestedt[3,*]

[1] Department of Biology, Stanford University, Stanford, CA 94305-5020, USA
[2] Department of Integrative Biology, University of California, Berkeley, CA 94720-3140, USA
[3] Department of Biodiversity Informatics and Genetics, Swedish Museum of Natural History, 10405 Stockholm, Sweden
[4] Department of Biology and School of Informatics, Computing, and Engineering, Indiana University, IN 47405, USA
[5] Department of Evolutionary Biology (EBC), Uppsala University, 75236 Uppsala, Sweden
[6] Department of Bio and Health Informatics, Technical University of Denmark, 2800 Lyngby, Denmark
[7] Centre of Excellence for Omics-Driven Computational Biodiscovery, Faculty of Applied Sciences, Asian Institute of Medicine, Science and Technology, Kedah, Malaysia.
[8] Department of Ornithology, American Museum of Natural History, New York, NY 10024, USA

* Corresponding authors: Stefan Prost (stefan.prost@berkeley.edu), Martin Irestedt (martin.irestedt@nrm.se)

Abstract

The diverse array of phenotypes and courtship displays exhibited by the birds-of-paradise have long fascinated scientists and laymen alike. Remarkably, almost nothing is known about the genomics of this iconic radiation. There are 41 species in 16 genera currently recognized within the birds-of-paradise family (*Paradisaeidae*), most of which are endemic to the island of New Guinea. In this study, we sequenced genomes of representatives from all five major clades within this family to characterize genomic changes that may have played an important role in the evolution of the group's extensive phenotypic diversity. We found genes important for coloration, morphology and feather development to be under positive selection. GO enrichment of positively selected genes in the birds-of-paradise showed an enrichment for collagen, glycogen synthesis and regulation, eye development and other categories. In the core birds-of-paradise, we found GO categories for 'startle response' (response to predators) and 'olfactory receptor activity' to be enriched among the gene families expanding significantly faster compared to the other birds in our study. Furthermore, we found novel families of retrovirus-like retrotransposons active in all three *de novo* genomes since the early diversification of the birds-of-paradise group, which could have potentially played a role in the evolution of this fascinating group of birds.

Keywords: *birds-of-paradise, comparative genomics,* gene gain-loss, positive selection, genome structure

Background

'Every ornithologist and birdwatcher has his favourite group of birds. Frankly, my own are the birds of paradise and bowerbirds. If they do not rank as high in world-wide popularity as they deserve it is only because so little is known about them.'

Ernst Mayer (in Gilliard 1969 [1])

The spectacular morphological and behavioral diversity found in birds-of-paradise (*Paradisaeidae*) form one of the most remarkable examples in the animal kingdom of traits that are thought to have evolved via forces of sexual selection and female choice. The family is comprised of 41 recognized species divided into 16 genera [2], all of which are confined to the Australo-Papuan realm. The birds-of-paradise have adapted to a wide variety of habitats ranging from tropical lowlands to high-altitude mountain forests [3] and in the process acquired a diverse set of morphological traits, some of which specifically fit their ecology and behavior. Some species are sexually monomorphic and crow-like in appearance with simple mating systems, whereas others have complex courtship behaviors and display strong sexual dimorphism with males exhibiting elaborate feather ornaments that serve as secondary sexual traits [3]. As such, strong sexual and natural selection have likely acted in concert to produce the exquisite phenotypic diversity among members the *Paradisaeidae*.

While having attracted substantial attention from systematists for centuries, the evolutionary processes and genomic mechanisms that have shaped these phenotypes remain largely unknown. In the past, the evolutionary history of birds-of-paradise has been studied with morphological data [1], molecular distances [4, 5], and a single mitochondrial gene [6], but the conclusions have been largely incongruent. The most comprehensive phylogenetic study at present includes all 41 species and is based on DNA-sequence data from both mitochondrial (cytochrome B) and nuclear genes (ornithine decarboxylase introns ODC6 and ODC7) [7]. This study suggests that the birds-of-paradise started to diverge during late Oligocene or early Miocene and could be divided into five main clades. The sexually monomorphic genera *Manucodia*, *Phonygammus*, and *Lycocorax* form a monophyletic clade (Clade A; Fig. 1 in Irestedt et al. 2009 [7]), which is suggested to be sister to the other four clades that include species with more or less strong sexual dimorphism (here referred to as "core birds-of-paradise"). Among the latter four clades, the genera *Pteridophor*a and *Parotia* are suggested to form the earliest diverging clade (Clade B; Fig. 1 in Irestedt et al. 2009 [7]), followed by a clade consisting of the genera *Seleucidis*, *Drepanornis*, *Semioptera, Ptiloris*, and *Lophorina* (Clade C; Fig. 1 in Irestedt et al. 2009 [7]). The last two sister clades are formed by *Epimachus*, *Paradigalla*, and *Astrapia* (Clade D; Fig. 1 in Irestedt et al. 2009 [7]), and *Diphyllodes*, *Cicinnurus*, and *Paradisaea* (Clade E;

Fig. 1 in Irestedt et al. 2009 [7]), respectively. In general, the phylogenetic hypothesis presented in Irestedt et al. (2009) [7] receives strong branch support (posterior probabilities), but several nodes are still weakly supported and there is incongruence among gene trees. Recently, Irestedt and colleagues [8] and Scholes and Laman [9] argued for the Superb birds-of-paradise to be split into several species, based on genetics, morphology and courtship behavior. Thus, while preliminary genetic analyses have outlined the major phylogenetic divisions, the interspecific relationships remain largely unresolved.

Birds-of-paradise are most widely known for their extravagant feather types, coloration and mating behaviors [3]. In addition, they also exhibit an array of bill shapes (often specialised on foraging behavior), and body morphologies and sizes [3]. Ornament feather types include 'wire-type' feathers (e.g. Twelve-wired bird-of-paradise (*Seleucidis melanoleuca*)), erectile head plumes (e.g. King of Saxony bird-of-paradise (*Pteridophora alberti*)), significantly elongated tail feathers (e.g. Ribbon-tailed Astrapia (*Astrapia mayeri*)) or finely-filamental flank plumes (e.g. Lesser bird-of-paradise (*Paradisaea minor*); see Frith and Bheeler 1998 [3]). Feathers and coloration are crucial components of their mating displays (see Discussion below). Polygynous birds-of-paradise show aggregated leks high in tree tops, less aggregated leks on lower levels or the forest floor (often exploded leks), and even solitary mating displays [3].

The array of extravagant phenotypes found in birds-of-paradise makes them an interesting model to study evolution. However, fresh tissue samples from birds-of-paradise are extremely limited and currently only about 50% of all species are represented in biobanks. Fortunately, the current revolution in sequencing technologies and laboratory methods does not only enable us to sequence whole-genome data from non-model organisms, but it also allows us to harvest genome information from specimens in museum collections [10]. Only recently, have these technological advances enabled researchers to investigate genome-wide signals of evolution using comparative and population genomic approaches in birds [11-14].

In the current study, we made use of these technological advances to generate *de novo* genomes for three birds-of-paradise species and re-sequenced the genomes of two other species from museum samples. Using these genomes, we were able to contrast the trajectory of genome evolution across passerines and simultaneously evaluate which genomic features have evolved during the radiation of birds-of-paradise. We identified a set of candidate genes that most likely have contributed to the extraordinary diversity in phenotypic traits found in birds-of-paradise.

Results

Assembly and gene annotation

We *de novo* assembled the genomes of *Lycocorax pyrrhopterus*, *Ptiloris paradiseus* and *Astrapia rothschildi* using paired-end and mate pair Illumina sequence data, and performed reference based mapping for *Pteridophora alberti* and *Paradisaea rubra*. Scaffold N50 ranged from 4.2 Mb (L. *pyrrhopterus*) to 7.7 Mb (*A. rothschildi*), and the number of scaffolds from 2,062 (*P.*

paradiseus) to 3,216 (*L. pyrrhopterus*; Supplementary Table S1). All assemblies showed a genome size around 1 Gb. BUSCO2 [15] scores for complete genes (using the aves_odb9 database) found in the respective assemblies ranged from 93.8% to 95.1%, indicating a high completeness (Supplementary Table S2). Next we annotated the genomes using homology to proteins of closely related species as well as *de novo* gene prediction. Gene numbers ranged from 16,260 (*A. rothschildi*) to 17,269 (*P. paradiseus;* see Supplementary Table S3).

Repeat evolution in birds-of-paradise

Our repeat annotation analyses (Supplementary Table S4) suggest that the genomes of birds-of-paradise contain repeat densities (~7%) and compositions (mostly chicken repeat 1 (CR1) long interspersed nuclear elements (LINEs), followed by retroviral long terminal repeats (LTRs)) well within the usual range of avian genomes [16]. However, we identified 16 novel LTR families (Supplementary Table S5) with no sequence similarity to each other or to LTR families known from in-depth annotations of chicken, zebra finch, and collared flycatcher [17, 18]. Interestingly, we find that activity of CR1 LINEs ceased recently in the three birds-of-paradise and was replaced by activity of retroviral LTRs (Fig. 1). The inferred timing of the TE (Tandem element) activity or accumulation peak (Fig. 1) corresponds to the radiation of birds-of-paradise (inferred in Irestedt et al. 2009 [7]). We also found that the genome assembly of *Lycocorax pyrrhopterus* exhibits slightly higher repeat densities than those of the two other birds-of-paradise (Supplementary Table S4) and slightly more recent TE activity (Fig. 1). A possible explanation for this is that this is the only female bird-of-paradise assembly, thus containing the female-specific W chromosome which is highly repetitive [16].

Genome synteny to the collared flycatcher

We found strong synteny of the three *de novo* assembled birds-of-paradise genomes (*Lycocorax pyrrhopterus*, *Ptiloris paradiseus, Astrapia rothschildi*) to that of the collared flycatcher (Fig. 2 and Supplementary Figures S1-3). Only a few cases were found where scaffolds of the birds-of-paradise genomes mapped to different chromosomes in the collared flycatcher genome.

Phylogeny

We found 4,656 one-to-one orthologous genes to be present in all eight sampled bird genomes (5 birds-of-paradise and 3 outgroup songbirds). A phylogeny inferred using these orthologs shows a topology with high bootstrap scores (Fig. 3 and Supplementary Figure S4). However, the sole use of bootstrapping or Bayesian posterior probabilities in analyses of large scale data sets has come into question in recent years [19]. Studies based on genome-wide data have shown that phylogenetic trees with full bootstrap or Bayesian posterior probability support can exhibit different topologies (e.g. Jarvis et al. 2014 [20] and Prum et al. 2015 [21]; discussed in Suh 2016 [19]). Thus, next we performed a concordance analysis by comparing gene trees for the 4,656 single-copy orthologs to the inferred species topology. We find strong concordance for the older splits in our phylogeny (see Supplementary Figure S4). However, the splits between Ptiloris and its sister clade, which contains Astrapia and Paradisaea, and the split between Astrapia and Paradisaea itself showed much lower concordance values, 0.31 and 0.26, respectively. Only ~10% of the gene trees exactly matched the topology of the inferred species tree

and we find an average Robinson-Foulds distance of 3.92 for all gene trees compared to the species tree (Supplementary Table S6). A Robinson-Foulds distance of 0 would indicate that the two tree topologies (species to gene tree) are identical. The highest supported species tree topology (Fig. 3 and Supplementary Figure S4) is identical to the birds-of-paradise species tree constructed in Irestedt et al. 2009 [7]. Overall, we find that the birds-of-paradise form a monophyletic clade, with the crow (*Corvus cornix*) being the most closely related sister taxa, in most gene trees (74%). Within the birds-of-paradise clade, we further distinguish a core birds-of-paradise clade, which consist of 4 of the 5 species in our sample (excluding only the paradise crow, *Lycocorax pyrrhopterus*).

Positive selection in the birds-of-paradise

We carried out positive selection analyses using all previously ascertained orthologous genes (8,134 genes present in at least seven out of the eight species) on the branch leading to the birds-of-paradise. First, we investigated saturation by calculating pairwise dN/dS ratios. The inferred values did not show any signs of saturation (Supplementary Table S7). To infer positive selection on the branch of the birds-of-paradise, we used the BUSTED model in HyPhy (similar to branch-sites model; [22]). We found 178 genes to be under selection (p value < 0.05; gene symbol annotation for 175 of the 178 genes can be found in Supplementary Table S8). GO enrichment resulted in 47 enriched GO terms using a 0.05 FDR cutoff (262 before correction; Supplementary Table S9). GO analysis showed enrichment of several categories related to collagen, skeletal and feather development, eye development, and glycogen synthesis and regulation (Supplementary Table S9).

Gene gain and loss

We identified 9,012 gene families across all 8 species. Using CAFE [23] we inferred 98 rapidly evolving families within the birds-of-paradise clade. Supplementary Table S10 summarizes the gene family changes for all 8 species (also see Fig. 3). Zebra finch had the highest average expansion rate across all families at 0.0916, while the hooded crow had the lowest average expansion rate at -0.1724, meaning that they have the most gene family contractions. Gene gain loss rates can be found in Supplementary Table S11. Next, we tested for enrichment of GO terms in the set of families rapidly evolving in the birds-of-paradise clade. Gene families were assigned GO terms based off the Ensembl GO predictions for flycatcher and zebra finch. In all, we were able to annotate 6,350 gene families with at least one GO term. Using a Fisher's exact test on the set of 98 rapidly evolving families in the birds-of-paradise, we find 25 enriched GO terms in 20 families (FDR 0.05; Supplementary Table S12). All the gene gain and loss results can be found online (https://cgi.soic.indiana.edu/~grthomas/cafe/bop/main.html).

Discussion

Renowned for their extravagant plumage and elaborate courtship displays, the birds-of-paradise are among the most prominent examples of how sexual selection can give rise to extreme phenotypic diversity. Despite extensive work on systematics and a long-standing interest in the evolution of their different mating behaviors, the genomic changes that underlie this phenotypic ra-

diation have received little attention. Here, we have assembled representative genomes for the five main birds-of-paradise clades and characterized differences in genome evolution within the family and relative to other avian groups. We reconstructed the main structure of the family phylogeny, uncovered substantial changes in the TE landscape and identified a list of genes under selection and gene families significantly expanded or contracted that are known to be involved with many phenotypic traits for which birds-of-paradise are renowned. Below, we discuss these different genomic features and how they might have contributed to the evolution of birds-of-paradise.

Genome synteny and phylogeny

We found genome synteny (here in comparison to the collared flycatcher) to be highly conserved for all three *de novo* assembled genomes (Fig. 2 and Supplementary Figures S1-3). Only a few cases were recorded where regions of scaffolds of the birds-of-paradise genomes aligned to different chromosomes of the collared flycatcher. These could be artifacts of the genome assembly process or be caused by chromosomal fusions/fissions. Passerine birds show variable numbers of chromosomes (72-84 [16]). However, while passerines' chromosome numbers do not vary as much as other groups', such as Charadriiformes (shorebirds, 40-100 [16]), they still show frequent fissions and fusions of macro- and microchromosomes. Apart from these fission and fusion events, studies have shown a high degree of genome synteny even between Galloanseres (chicken) and Neognathae (approx. 80-90 mya divergence, reviewed in Ellegren 2010 [24]; Poelstra et al. 2014 [11]). However, genomes with higher continuity, generated with long-read technologies or using long-range scaffolding methods (such as HiC [25]), or a combination thereof, will be needed to get a more detailed view of rearrangements in genomes of birds-of-paradise.

Our analyses reconstructed a phylogenetic tree topology congruent with the one presented in Irestedt et al. 2009 [7] (Fig. 3 and Supplementary Figure 4). However, while bootstrapping found full support for the topology of the species tree, congruence analysis found high discordance for the two most recent branches (*Ptiloris* and its sister clade (*Astrapia* and *Paradisaea*) and the split between *Astrapia* and *Paradisaea*). Furthermore, we found the highest supported tree topology to be based on only 10% of all gene trees (Supplementary Table S6). This could be caused by incomplete lineage sorting (ILS), which refers to the persistence of ancestral polymorphisms across multiple speciation events [26]. Jarvis et al. 2014 [20] and Suh et al. 2015 [27] showed that ILS is a common phenomenon on short branches in the bird Tree of Life. Another possibility could be hybridization, a phenomenon frequently recorded in birds-of-paradise [3]. Overall, most gene tree topologies (74%) support the monophyly for the birds-of-paradise and the core birds-of-paradise clades.

Repeats and their possible role in the evolution of birds-of-paradise

A growing body of literature is emerging that proposes an important role of TEs in speciation and evolution (see e.g. Feschotte 2008 [28], Oliver and Greene 2009 [29]). Bursts of TE activity are often lineage and species-specific, which highlights their potential role in speciation [30].

This is further supported by the fact that TE activity bursts often correlate with the speciation timing of the respective species or species group [31]. Similarly, we find a burst of TE activity within all three *de novo* assembled genomes (*Lycocorax pyrrhopterus*, *Ptiloris paradiseus*, *Astrapia rothschildi*) dating back to about 24 mya (Fig. 1). The timing fits the emergence and radiation of birds-of-paradise (see Fig 3). The fact that we found 16 novel families of retroviral LTRs suggests multiple recent germline invasions of the birds-of-paradise lineage by retroviruses. The recent cessation of activity of CR1 LINEs and instead recent activity of retroviral LTRs (Fig. 1) is in line with similar trends in collared flycatcher and hooded crow [16, 17]. This suggests that recent activity of retroviral LTRs might be a general genomic feature of songbirds, however, with different families of retroviruses being present and active in each songbird lineage. It is thus likely that the diversification of birds-of-paradise was influenced by lineage specificity of their TE repertoires through retroviral germline invasions and smaller activity bursts.

Coloration, feather and skeletal development in birds-of-paradise

The diverse array of color patterns exhibited by birds-of-paradise involve both pigmentary and structural coloration mechanisms. Coloration via pigmentation is achieved by pigment absorption of diffusely scattered light in a specific wavelength range. Pigments such as carotenoids are frequently associated with red and yellow hues in birds, whereas light absorption by various classes of melanin give rise to black plumage features common to many birds-of paradise [32]. On the other hand, structural coloration is caused by light reflection of quasiordered spongy structures of the feather barbs and melanosomes in feather barbules [33, 34]. The plumages of male birds-of-paradise feature both coloration types to various degrees, and some species such as the Lawes' parotia (*Parotia lawesii*) use angular-dependent spectral color shifts of their structural feathers in their elaborate display rituals to attract females [35, 36]. Most core birds-of-paradise show a strong sexual dimorphism, with highly ornamented males and reduced ornamentation in females [3]. Dale and colleagues recently showed that sexual selection on male ornamentation in birds has antagonistic effects, where male coloration is increasing, while females show a strong reduction in coloration [37]. This is very apparent in polygynous core birds-of-paradise, where females between species and sometimes even between genera look highly similar. Given their strong sexual dimorphism and its important role in mating success, we would expect genes important for coloration, morphology and feather structure to be under strong selection in the birds-of-paradise. In accordance with this prediction, we found several GO categories enriched in positively selected genes in birds-of-paradise that could be associated with these phenotypes.

One such gene is ADAMTS20, which is crucial for melanocyte development. ADAMTS20 has been shown to cause white belt formation in the lumbar region of mice [38]. Nonsense or missense mutations in this gene disrupt the function of KIT, a protein that regulates pigment cell development [38]. In mammals and birds pigment patterns are exclusively produced by melanocytes. Thus, this gene could be a strong candidate for differential coloration in the birds-of-paradise. Another gene under positive selection with a potential role in coloration is ATP7B. It is a copper-transporting P-type ATPase and thought to translate into a melanosomal protein (see

Bennett and Lamoreux 2003 [39] for a review). Copper is crucial for melanin synthesis because tyrosinase contains copper and thus ATP7B might play a crucial role in pigment formation.

Genes in GO categories involving collagen and the extracellular matrix are likely affecting morphology (feather, craniofacial and skeletal muscle development) in birds-of-paradise (Supplementary Table S9). Several genes under positive selection fall into these GO categories. FGFR1 (Fibroblast growth factor receptor 1) is implicated in feather development [40]. In humans it has further been shown to be involved in several diseases associated with craniofacial defects (OMIM; http://www.ncbi.nlm.nih.gov/omim/). ALDH3A2 (aldehyde dehydrogenase 3 family member A2), a membrane-associated protein and SPECC1L are implicated in craniofacial disorders (e.g. Van Der Woude Syndrome) in humans [41] and ALDH3A2 has been listed as a candidate gene for beak development in birds [12]. GAB2 (GRB2-associated-binding protein 2) is an important gene in osteoclastogenesis and bone homeostasis [42] (bone remodeling). PAPSS2 (Bifunctional 3'-phosphoadenosine 5'-phosphosulfate synthetase 2) plays an important role in cartilage development [43]. Similarly, DCST2 (*DC-STAMP domain containing 2)* is an important regulator of osteoclast cell-fusion in bone homeostasis [44], and has been shown to be associated with body length in early life and height in adulthood [45]. MYF5 (Myogenic factor 5) has been shown to be important for skeletal muscle phenotype and initiates the myogenic program [46] (muscle tissue formation). APOBEC2 seems to play a role in muscle development (skeletal and heart muscle) in chickens [47].

APOBECs and their potential role in the immune system

Intriguingly, APOBECs have also been shown to have important functions in the immune systems of vertebrates, where they act as restriction factors in the defense against a range of retroviruses and retrotransposons [48, 49]. Functioning as cytosine deaminases they act against endogenous retroviruses (ERVs), especially Long terminal repeat retrotransposons (LTR) by interfering with the reverse transcription and by hypermutating retrotransposon DNA. A recent study on 123 vertebrates showed that birds have the strongest hypermutation signals, especially oscine passerines [50] (such as zebra finch and medium ground finch). This study also demonstrated that edited retrotransposons may preferentially be retained in active regions of the genome, such as exons, promoters, etc. (hypermutation decreases their potential for mobility). Thus, it seems very likely that retrotransposon editing via APOBECs has an important role in the innate immunity of vertebrates as well as in genome evolution. Congruently, we found a burst in recent activity of retroviral LTRs in the genomes of birds-of-paradise, a similar signal was further found in other passerines [16, 17]. This could also explain the why we found APOBEC2 to be under positive selection.

In concert, the inferred genes under positive selection and the results of the GO category enrichment analyses indicate that positive selection has played a role in shaping morphological phenotypes of the birds-of-paradise and targeted developmental genetics studies may further elucidate their specific roles in this family.

Sensory system in the birds-of-paradise

Visual system

We also found two GO categories associated with eye development and function to be enriched for positively selected genes in birds-of-paradise, namely “retina development in camera-type eye” and “photoreceptor outer segment”. Genes that showed positive selection and are known to have critical roles in eye function and development include CABP4, NR2E3, IMPG1, GNB1, AKAP13, MGARP, CDADC1 and MYOC. For example, CaBP4 is a member of a subfamily of calmodulin-like neuronal Ca2þ-binding proteins (CaBP1-8) and is essential for normal photoreceptor synaptic function via continuous release of neurotransmitter in retinal photoreceptor cells [51]. NR2E3, a photoreceptor-specific nuclear receptor is a transcription factor important for retinal development [52]. Transcription analysis of MYOC indicates a structural or functional role of myocilin in the regulation of aqueous humor outflow that may influence intraocular pressure, and in the optical nerve [53].

There are no single obvious explanations for selection on vision in birds-of-paradise. Evidence for co-evolution between coloration and vision in birds is weak (see e.g. Lind et al. 2017 [54], Price 2017 [55], but see Mundy et al. 2016 [56] and Bloch 2015 [57]). Another phenotype that might be associated with selection on vision is the diverse array of mating displays in some core birds-of-paradise. Many species, such as the Lawes’ parotia (*Parotia lawesii*) modify color by changing the angle of the light reflection [35, 36], which requires the visual system to be able to process the fine nuances of these color changes. However, the fact that (color) vision serves many purposes (including e.g. foraging, etc.) makes it very difficult to establish co-evolution between coloration and color vision [54]. We can thus only speculate at this point about the potential role of coloration or mating displays in the selection of vision genes found in birds-of-paradise.

Olfactory system

Another often overlooked sensory system in birds is odor perception. Olfactory receptors (ORs) are important in odor perception and detection of chemical cues. In many animal taxa, including birds, it has been shown that olfaction is crucial to identify species [58], relatedness [59], individuals [60], as well as for mate choice [61] and in foraging [62]. In concordance with previous studies we found this gene family to expand rapidly in the zebra finch [63]. Even more so, the zebra finch showed the strongest expansion (+17 genes). Furthermore, we find a rapid expansion on the branch leading to the core birds-of-paradise (+5 genes) and further in *Astrapia* (+6 genes). Interestingly, olfactory receptor genes show rapid contractions in the paradise crow (-6 genes), the hooded crow (-9 genes) and the collared flycatcher (-5 genes). This is in line with a study that suggested poor olfactory development in the Japanese jungle crow (*Corvus macrorhynchos*) [64]. Olfactory could serve many functions in birds-of-paradise e.g. in species recognition (to avoid extensive hybridization), individual recognition, mating or foraging (given their extensive diet breadth), among others.

Startle response and adult locomotory behavior

Startle response is an important behavioral trait. It is the ability to quickly react to the presence of a stimuli, such as the presence of predators. It could be crucial for core birds-of-paradise that show extravagant lekking behavior, arguably especially for those taxa that congregate at large leks at highly visible places. Being highly visible means that they need to be able to look out for predators and react to them quickly, and indeed Frith & Beehler 1998 [3] mention that lekking birds-of-paradise appear to be constantly on the lookout for predators. We find a gene family associated with startle response and adult locomotory behavior to be evolving significantly faster than under a neutral model on the branch leading the core birds-of-paradise (+5 genes). It is even further expanded in the genus *Paradisaea* (+3 genes). Interestingly, species of the genus *Paradisaea* have aggregated leks high in emergent trees and thus may be more visible to the numerous birds of prey that inhabit the region, while most other core birds-of-paradise display on lower levels in trees or on the forest floor and have less aggregated leks (exploded lek) or solitary display [3]. This gene family is contracted in the two outgroups, the zebra finch (-4 genes) and the collared flycatcher (-2 genes), as well as the monochromatic, non-lekking Paradise crow (-1 genes). We found no expansion or contraction in the hooded crow genome.

Other positively selected genes and enriched GO categories

Other interesting genes under positive selection include CTSD (Cathepsin D), a gene that has been shown to play a key (enzymatic) role in yolk production in chicken [65]. CTSD is primarily important for egg yolk and egg weight [65, 66]. We also found several genes important for sexual development to be under positive selection. These include CBX2, SPAG16, TAF4B, SPATA5L1 and DCST2. CBX2 (Chromobox homolog 2) has been shown to determine sex in humans, maybe even more so than X/Y chromosomes [67]. It is essential for the expression of SRY (sex determining region on the Y chromosome), which determines sex in most eutherian mammals [68]. Other genes include SPAG16 (Sperm-associated antigen 16) and STRA8 (Stimulated By Retinoic Acid 8), both of which are essential for spermatogenesis [69], and TAF4B (Transcription initiation factor TFIID subunit 4B), which is important for healthy ovarian aging and female fertility in mice and humans [70].

Interestingly, we found several GO categories related to glycogen synthesis and regulation to be enriched in the set of positively selected genes in birds-of-paradise (Supplementary Table S9). Genes under positive selection important for glycogen synthesis and regulation include SLC5A9, G6PC2, AGL, B3GLCT, PHLDA3 and IDE. SLC5A9 (Solute Carrier Family 5 Member 9), also called SGLT4, is a glucose transporter [71]. G6PC2 (Glucose-6-phosphatase 2) is involved in catalyzing the hydrolysis of glucose-6-phosphate, the terminal step in gluconeogenic and glycogenolytic pathways, which allow glucose to be released into the bloodstream [72]. AGL (amylo-1,6-glucosidase) is a glycogen debranching enzyme[99], which facilitates the breakdown of glycogen (storage of glycogen in the body). We also found IDE (insulin degrading enzyme) to be under positive selection in birds-of-paradise. This gene is a large zinc-binding protease and degrades the B chain of insulin [73]. In birds, glucose is utilized in a variety of functions, with the main one being energy production through cellular oxidation, glycogen synthesis,

etc. (see Braun and [74] 2008 for a review). Interestingly, birds maintain higher levels of plasma glucose than other vertebrates of similar body mass, but seem to store very little as glycogen [74]. On the contrary to other vertebrates, plasma glucose levels are insensitive to insulin in birds (see e.g. Sweazea et al. 2006 [74]). It thus seems surprising that we found a significant enrichment of positively selected genes involved in 'positive regulation of glucose import in response to insulin stimulus' in birds-of-paradise. On the other hand, it appears that gluconeogenesis plays an important role in maintenance of plasma glucose levels in birds [75]. Furthermore, it has been shown that in some birds, such as pigeons, blood glucose levels are significantly increased during courtship and mating, a time of significant energy requirement [76].

High plasma glucose levels, high metabolic rates and high body temperatures should increase oxidative stress in birds [77]. However, birds have developed efficient mechanisms to prevent tissue damage of oxidative stress (see e.g. Holmes et al. 2001 [77]). Furthermore, studies have shown that mitochondria in different bird tissues produce much lower levels of reactive oxygen [78]. In addition, they show higher levels of antioxidants superoxide dismutase, catalase and glutathione peroxidase [78]. Intriguingly, we found a significant GO enrichment of 'glutathione peroxidase activity' in the set of positively selected genes in birds-of-paradise.

Beside energy storage, glycogen seems to have a function in the visual system of some birds. Several studies have shown a high concentration of glycogen B in lenses of flying birds [79]. The function of glycogen in lenses of flying birds is unknown, but a structural function, more specifically the maintenance of the refractive index of the lens, is suspected [79]. Castillo and colleagues were able to detect high concentrations of glycogen in pigeon and dove, but not the chicken [79] (which they classify as a ground-running bird).

Conclusions

We found several genes with known function in coloration, feather, and skeletal development to be under positive selection in birds-of-paradise. This is in accordance with our prediction that phenotypic evolution in birds-of-paradise should have left strong genomic signatures. Furthermore, positively selected genes were enriched for GO terms associated with collagen and extracellular matrix development. While these gene categories all are obvious candidates for being important in the evolution of birds-of-paradise's phenotypic and behavioral diversity, we also found enrichment in other positively selected genes that are not as straight forward to explain. These include eye development and function, glycogen synthesis and regulation, and glutathione peroxidase activity. Gene gain loss analyses further revealed significant expansions in gene families associated with 'startle response' (response to predators) and olfactory function. On the genome level, we found indications of a highly conserved synteny between birds-of-paradise and other passerine birds, such as the collared flycatcher. Similar to other passerine groups we also found strong signatures of recent activity of novel retroviral LTRs in the genomes. Birds-of-paradise show positive selection on APOBEC2, likely to counteract deleterious effects of LTRs, by decreasing their activity.

Although recent advances in documenting the phenotypic and behavioral diversity in the birds-of-paradise continues to generate intense interest in this model system, we still have very limited understanding of the processes that have shaped their evolution. Here, we provide a first glimpse into genomic features underlying the diverse array of phenotypes found in birds-of-paradise. However, more in depth analyses will be needed to verify a causal relationship between signatures of selection in the birds-of-paradise genome and the unique diversity of phenotypic traits, or to investigate genome structure changes with higher resolution. Fortunately, technologies keep advancing, and along with decreasing costs for sequencing, we will soon be able to gain more information about this fascinating, but understudied family of birds.

Data description and Analyses

Sampling and DNA extraction

For the three *de novo* genome assemblies, *Lycocorax pyrrhopterus* (ZMUC149607; collected 2013, Obi Island, Indonesia), *Ptiloris paradiseus* (ANWC43271; collected 1990, New South Wales, Australia), and *Astrapia rothschildi* (KU Birds 93602; collected 2001, Morobe Province, Papua New Guinea) DNA was extracted from fresh tissue samples using the Qiagen QIAamp DNA Mini Kit according to the manufacturer's instructions. The *de novo* libraries with different insert sizes (see below) were prepared by Science for Life Laboratory, Stockholm. For the two re-sequenced genomes, *Pteridophora alberti* (NRM571458; collected 1951, Eastern Range, New Guinea) and *Paradisaea rubra* (NRM700233; collected 1949, Batanta Island, New Guinea), we sampled footpads and extracted DNA using the Qiagen QIAamp DNA Micro Kit to the manufacturer's instructions. We applied precautions for working with museum samples described in Irestedt et al., (2006) [80]. Sequencing libraries for these two samples were prepared using the protocol published by Meyer and Kircher, (2010) [81]. This method was specifically developed to generate sequencing libraries for low input DNA, showing DNA damage typical for museum or ancient samples.

Genome Sequencing, Assembly, and Quality Assessment

We prepared two paired-end (overlapping and 450bp average insert size) and two mate pair libraries (3kb and 8kb average insert size) for each of the three *de novo* assemblies (*Ptiloris paradiseus, Astrapia rothschildi*, and *Lycocorax pyrrhopterus)*. All libraries, for the *de novo* and the reference-based mapping approaches were sequenced on a HiSeq2500 v4 at SciLife Stockholm, Sweden. We generated 2 lanes of sequencing for each *de novo* assembly and pooled the two reference-based samples on one lane. We first assessed the read qualities for all species using the program FastQC [82]. For the three species, *Ptiloris paradiseus, Astrapia rothschildi*, and *Lycocorax pyrrhopterus* we then used the *preqc* [83] function of the SGA [84] assembler to (1) estimate the predicted genome size, (2) find the predicted correlation between k-mer sizes and N50 contig length and (3) assess different error statistics implemented in *preqc*. For *Ptiloris paradiseus, Astrapia rothschildi*, and *Lycocorax pyrrhopterus* reads were assembled using Allpaths-LG [85]. To improve the assemblies, especially in repeat regions, GapCloser (part of the SOAPdenovo package [86]) was used to fill in gaps in the assembly. Assemblies were then compared using CEGMA [87] and BUSCO2 [15]. We added BUSCO2 scores for better compari-

sons at a later stage of the project. For the reference-based mapping, we mapped all reads back to the *Ptiloris paradiseus* assembly using BWA [88] (mem option), the resulting sam file was then processed using samtools [89]. To do so, we first converted the sam file generated by BWA to the bam format, then sorted and indexed the file. Next we removed duplicates using Picard (http://broadinstitute.github.io/picard/) and realigned reads around indels using GATK [90]. The consensus sequence for each of the two genomes was then called using ANGSD [91] (using the option -doFasta 3). [Genomes will be deposited in GenBank]

Repeat Annotation

We predicted lineage-specific repetitive elements *de novo* in each of the three birds-of-paradise genome assemblies using RepeatModeler v. 1.0.8 [92]. RepeatModeler constructs consensus sequences of repeats via the three complementary programs RECON [93], RepeatScout [94], and Tandem Repeats Finder [95]. Next, we merged the resultant libraries with existing avian repeat consensus sequences from Repbase [96] (mostly from chicken and zebra finch), and recent in-depth repeat annotations of collared flycatcher [97, 98] and hooded crow [99]. Redundancies among the three birds-of-paradise libraries, and between these and existing avian repeats were removed using the ReannTE_mergeFasta.pl script (https://github.com/4ureliek/ReannTE/). For *Lycocorax pyrrhopterus* repeats, we manually inspected the RepeatModeler library of consensus sequences for reasons reviewed in Platt et al. (2016) [100] and because *Lycocorax pyrrhopterus* was the most repeat-rich genome among the three birds-of-paradise. Manual curation was performed using standard procedures [27, 101], namely screening of each repeat candidate against the *Lycocorax pyrrhopterus* assembly using blastn [102], extracting the 20 best hits including 2-kb flanks, and alignment of these per-candidate BLAST hits to the respective consensus sequence using MAFFT v. 6 [103]. Each alignment was inspected by eye and curated majority-rule consensus sequences were generated manually considering repeat boundaries and target site duplication motifs. This led to the identification of 33 long terminal repeat (LTR) retrotransposon consensus sequences (including 16 novel LTR families named as 'lycPyrLTR*') and three unclassified repeat consensus sequences (Supplementary Table S5). We then used this manually curated repeat library of *Lycocorax pyrrhopterus* to update the aforementioned merged library of avian and birds-of-paradise repeat consensus sequences. Subsequently, all three birds-of-paradise genome assemblies were annotated via RepeatMasker v. 4.0.6 and '-e ncbi' [104] using this specific library (Supplementary Table S4). Landscapes of relative TE activity (i.e., the amount of TE-derived bp plotted against Kimura 2-parameter distance to respective TE consensus) were generated using the calcDivergenceFromAlign.pl and createRepeatLandscape.pl scripts of the RepeatMasker packages. To enhance plot readability, TE families were grouped into the subclasses "DNA transposon", "SINE", "LINE", "LTR", and "Unknown" (Fig. 1). We scaled the kimura substitution level with the four-fold degenerate mutation rate for Passeriformes (mean of 3.175 substitutions/site/million years for passerines sampled in Zhang et al. 2014 [13]) to obtain an estimate of the timing of the inferred repeat activity in million years (mya).

Genome Synteny

We also inferred genome architecture changes (synteny) between our three *de novo* assembled genomes and the chromosome-level assembly of the collared flycatcher. To do so, we first performed pairwise alignments using Satsuma [105] and then plotted the synteny using Circos plots [106]. More precisely, we first performed asynchronous 'battleship'-like local alignments using *SatsumaSynteny* to allow for time efficient pairwise alignments of the complete genomes. In order to avoid signals from tandem elements we used masked assemblies for the alignments. Synteny between genomes was then plotted using Circos and in-house perl scripts.

Gene Annotation

We masked repeats (only tandem elements) in the genome prior to gene annotation. Contrary to the repeat annotation step, we did not mask simple repeats in this approach. Those were later soft-masked as part of the gene annotation pipeline Maker2 [107], to allow for more efficient mapping during gene annotation.

Gene annotation was performed using *ab-initio* gene prediction and homology-based gene annotation. To do so we used the genome annotation pipeline Maker2 [107], which is able to perform all the aforementioned genome annotation strategies. Previously published protein evidence (genome annotations) from Zhang et al. 2014 [13] were used for the homology-based gene prediction. To improve the genome annotation we used CEGMA to train the *ab-initio* gene predictor SNAP [108] before running Maker2 [107]. We did not train the *de novo* gene predictor Augustus [109] because no training data set for birds was available.

Ortholog Gene Calling

In the next step we inferred orthologous genes using PoFF [110]. We included all five birds-of-paradise, as well as the hooded crow, the zebra finch and the collared flycatcher as outgroups. We ran PoFF using both the transcript files (in fasta format) and the transcript coordinates file (in gff3 format). The gff files were used (flag *–synteny*) to calculate the distances between paralogous genes to accurately distinguish between orthologous and paralogous genes. We then extracted the sequences for all one-to-one orthologs using a custom python script.

Next, we determined the number of genes with missing data in order to maximize the number of genes included in the subsequent analyses. For a gene to be included in our analyses, it had to be present in at least 75% of all species (7 out of 8 species), which resulted in a set of 8,134 genes. In order to minimize false positives in the subsequent positive selection analysis caused by alignment errors, we used the codon-based alignment algorithm of Prank [111] and further masked sites with possible alignment issues using Aliscore [112]. Aliscore uses Monte Carlo resampling within sliding windows to identify low-quality alignments in amino acid alignments (converted by the program). The identified potential alignment issues were then removed from the nucleotide alignments using ALICUT [113].

Intron Calling

In addition to exons, we also extracted intron information for the birds-of-paradise genomes (see Supplementary Table S3). To do so we used the extract_intron_gff3_from_gff3.py script (https://github.com/irusri/Extract-intron-from-gff3) to include intron coordinates into the gff file. We then parsed out all intron coordinates and extracted the intron sequences from the genomes

using the exttract_seq_from_gff3.pl script (https://github.com/irusri/Extract-intron-from-gff3). All introns for the same gene were then concatenated using a custom python script.

Phylogenetic analysis

The individual alignment files (we used exon sets without missing species, which resulted in 4,656 alignments) were then (1) converted to the phylip format individually, and (2) 200 randomly selected exon alignments were concatenated and then converted to phylip format using the catfasta2phyml.pl script (https://github.com/nylander/catfasta2phyml). We used the individual exon phylip files for gene tree reconstruction using RaxML [114] (using a GTR + G model). Subsequently, we binned the gene trees into a species tree and carried out bootstrapping using Astral [115, 116]. Astral applies a statistical binning approach to combine similar gene trees, based on an incompatibility graph between gene trees and then chooses the most likely species tree under the multi-species coalescent model. Astral does not provide branch lengths needed for calibrating phylogenetic trees (used for the gene gain/loss analysis). So, we subsampled our data, and constructed a ML tree based on 200 randomly chosen and concatenated exons using ExaML [117]. We then calibrated the species tree using the obtained branch lengths along with calibration points obtained from timetree.org using r8s [118]. These calibration points are the estimated 44mya divergence time between flycatcher and zebra finch and the 37mya divergence time between crow and the birds-of-paradise.

Next we performed a concordance analysis. First, we rooted the gene trees based on the outgroup (Flycatcher, zebra finch). Then, for each node in the species tree we counted the number of gene trees that contained that node and divided that by the total number of gene trees. We next counted the number of gene trees that support a given topology (see Supplementary Table S6) and further calculated the Robison-Foulds distance between gene trees using RaxML.

Inference of Positive selection

We inferred genes under positive selection using *dN/dS* ratios of 8,133 orthologs. First, we investigated saturation of synonymous sites in the phylogenetic sampling using pairwise comparisons in CodeML [119]. The pairwise runmode of CodeML estimates *dN* and *dS* ratios using a ML approach between each species pair (Supplementary Table S7). We then investigated positive selection on the branch to the birds-of-paradise using the BUSTED model [22] (branch-site model) implemented in HyPhy [120]. The branch-site test allows for inference of positive selection in specific branches (foreground branches) compared to the rest of the phylogeny (background branches). The significance of the model comparisons was determined using likelihood-ratio tests (LRT). We did not perform multiple testing corrections, such as Bonferroni correction, due to the fact that branch-site tests result in an access of non-significant p-values, which violates the assumption of a uniform distribution in multiple testing correction methods such as the Bonferroni correction. The genes were then assigned gene symbols. To do so, we first extracted all the respective zebra finch or collared flycatcher GeneBank protein accessions. We then converted the accessions into gene symbols using the online conversion tool bioDBnet [121]. GO terms were obtained for the flycatcher assembly and assigned to orthologs that had a corresponding flycatcher transcript ID in Ensembl (7,305 genes out of 8,133). To determine enriched GO categories in positively selected genes, GO terms in genes inferred to have undergone

positive selection were then compared to GO terms in all genes (with a GO term) using Fisher's exact test with a false discovery rate cut-off of 0.05. We found 262 GO terms enriched in positively selected genes before FDR correction and 47 enriched after.

Gene Gain-Loss

In order to identify rapidly evolving gene families in the birds-of-paradise we used the peptide annotations from all five birds-of-paradise species, along with the three outgroup species in our analysis: *Corvus cornix* (crow)*, Taeniopygia guttata* (zebra finch)*, Ficedula albicus* (flycatcher). The crow genes were obtained from NCBI and the zebra finch and flycatcher genes were acquired from ENSEMBL 86 [122]. To ensure that each gene was counted only once, we used only the longest isoform of each protein in each species. We then performed an all-vs-all BLAST [102] search on these filtered sequences. The resulting e-values from the search were used as the main clustering criterion for the MCL program to group peptides into gene families [123]. This resulted in 13,289 clusters. We then removed all clusters only present in a single species, resulting in 9,012 gene families. Since CAFE requires an ultrametric time tree as input, we used r8s to smooth the phylogenetic tree with calibration points based on the divergence time of crow and the birds-of-paradise at 37mya and of flycatcher and zebra finch at 44mya [124].

With the gene family data and ultrametric phylogeny (Figure 3) as input, we estimated gene gain and loss rates (λ) with CAFE v3.0 [125]. This version of CAFE is able to estimate the amount of assembly and annotation error (ε) present in the input data using a distribution across the observed gene family counts and a pseudo-likelihood search. CAFE is then able to correct for this error and obtain a more accurate estimate of λ. We find an ε of about 0.01, which implies that 3% of gene families have observed counts that are not equal to their true counts. After correcting for this error rate, we find $\lambda = 0.0021$. This value for λ is considerably higher than those reported for other distantly related groups (Supplementary Table S11). GO terms were assigned to genes within families based on flycatcher and zebra finch gene IDs from Ensembl. We used these GO assignments to determine molecular functions that may be enriched in gene families that are rapidly evolving along the ancestral BOP lineage (Node BOP11 in Figure S1). GO terms in genes in families that are rapidly evolving along the BOP lineage were compared to all other GO terms using a Fisher's exact test (FDR cut-off of 0.05). We found 36 genes in 26 families to have enriched GO terms before FDR correction and 25 genes in 20 families after.

DATA AND SOFTWARE AVAILABILITY

All genomes will be deposited in GigaDB, and raw read data are currently deposited on NCBI (SRA archive). All results of the gene gain-loss analyses can be found online (https://cgi.soic.indiana.edu/~grthomas/cafe/bop/main.html).

Acknowledgement

We thank Australian National Wildlife Collection, CSIRO Sustainable Ecosystems (Leo Joseph) for tissue sample from *Ptiloris paradiseus*, Natural History Museum of Denmark, University of Copenhagen (Knud Jønsson and Jan Bolding) for tissue samples from *Lycocorax pyrrhopterus*, and Natural History Museum, and Biodiversity Institute, University of Kansas (Robert Moyle) for

tissue samples of *Astrapia rothschildi.* Daniel Osorio for helpful discussion of coloration and color vision in birds, and Nagarjun Vijay for help with the circos plots. MI and PGPE were supported by the Swedish Research Council (grant number 621-2013-5161 to PGPE and grant number 621-2014-5113 to MI). We also acknowledge support from Science for Life Laboratory, the National Genomics Infrastructure (NGI), Uppmax and the EvoLab at the University of California Berkeley for providing resources for massive parallel sequencing and computational infrastructure. The funders had no role in study design, data collection and analysis, decision to publish, or preparation of the manuscript.

Figures

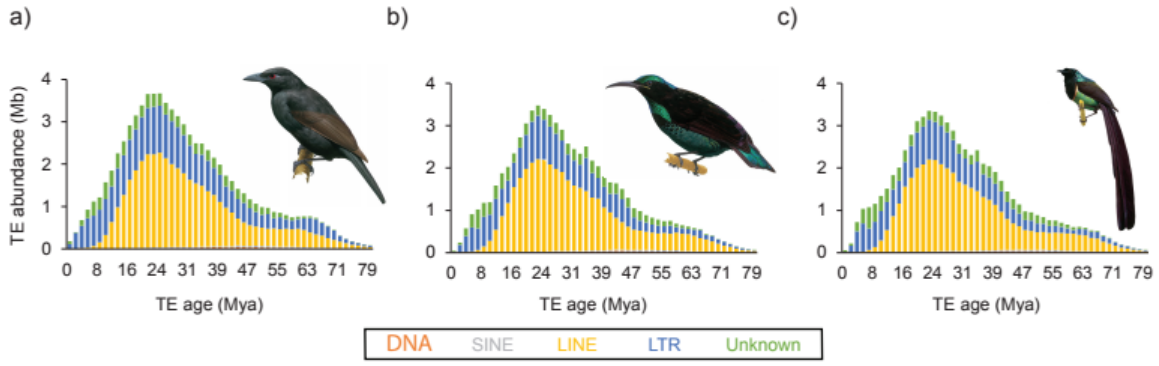

Figure 1: Repeat landscapes of *Astrapia rothschildi*, *Lycocorax pyrrhopterus*, and *Ptiloris paradisaeus*. Total amounts of TE-derived bp are plotted against relative age, approximated by per-copy Kimura 2-parameter distance to the TE consensus sequence and scaled using a four-fold degenerate mutation rate of Passeriformes of 3.175 substitutions/site/million years. TE families were grouped as “DNA transposons” (red), “SINEs” (grey), “LINEs” (yellow), “LTRs” (blue), and “Unknown” (green).

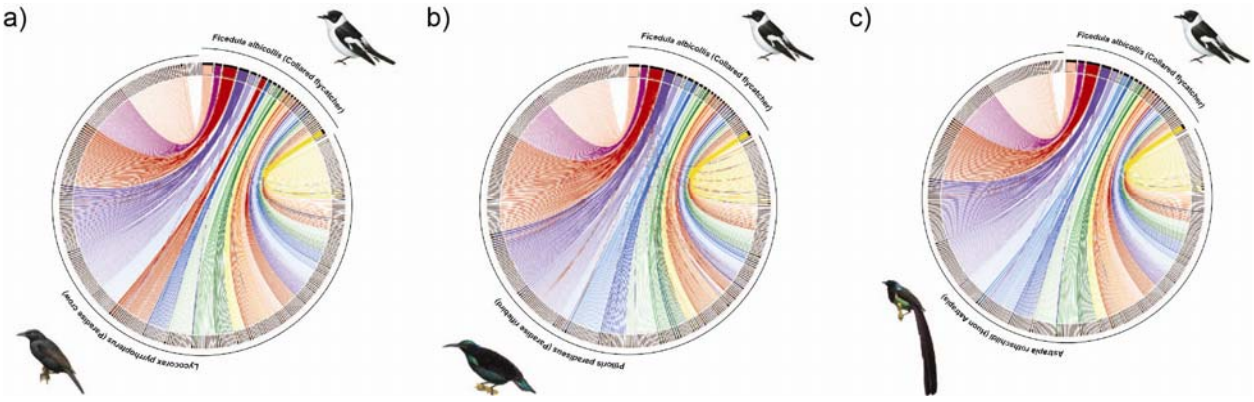

Figure 2: Chromosomal synteny plot between the collared flycatcher and (a) the paradise crow, (b) paradise riflebird and (c) the Huon Astrapia. The plot shows scaffolds bigger than 50kb and links (alignments) bigger than 2kb.

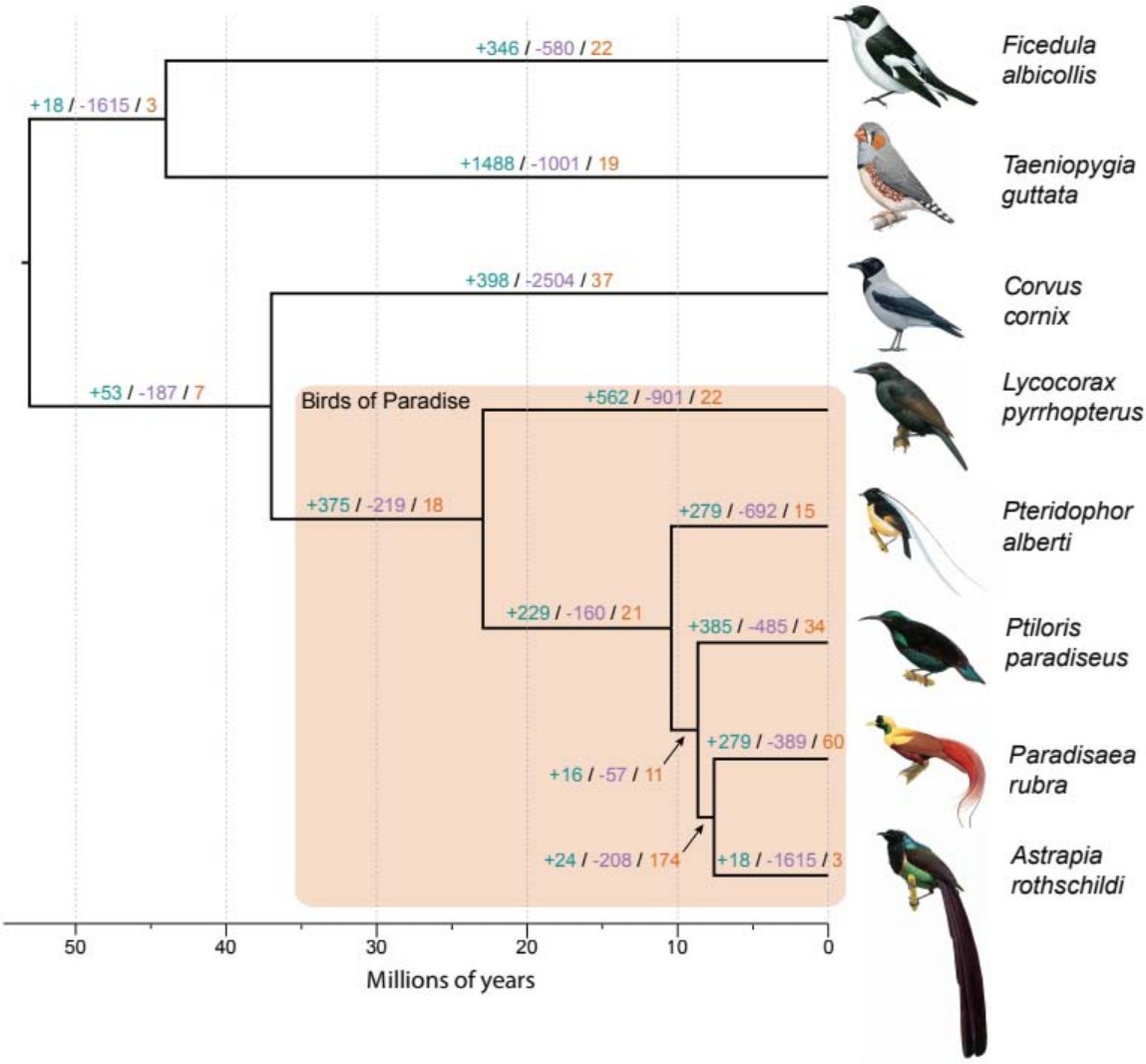

Figure 3: The birds-of-paradise phylogeny. The phylogenetic tree is based on ML and coalescent-based statistical binning of 4,656 genes, and scaled using the divergence times between crow and the birds-of-paradise, and zebra finch and flycatcher (obtained from Timetree.org) as calibration points. Branches are labeled as: # gene family expansions / # gene family contractions / # rapidly evolving gene families.

References

1. Gilliard, E.T. (1969). Birds of paradise and bower birds, (American Museum of Natural History).
2. Gill, F., and Donsker, D. (2017). IOC World Bird List (v 7.1). doi: 1014344/IOCML71. doi: 10.14344/IOC. (ML).
3. Frith, C., and Beehler, B. (1998). The Birds of Paradise. (Oxford University Press, Oxford, United Kingdom).
4. Cracraft, J. (1992). The species of the birds□of□paradise (Paradisaeidae): applying the phylogenetic species concept to a complex pattern of diversification. Cladistics *8*, 1-43.
5. Christidis, L., and Schodde, R. (1992). Relationships Among the Birds-of-Paradise (Paradisaeidae) and Bowerbirds (Ptilonorhynchidae)-Protein Evidence. Australian Journal of Zoology *40*, 343-353.
6. Nunn, G.B., and Cracraft, J. (1996). Phylogenetic relationships among the major lineages of the birds-of-paradise (Paradisaeidae) using mitochondrial DNA gene sequences. Molecular Phylogenetics and Evolution *5*, 445-459.
7. Irestedt, M., Jønsson, K.A., Fjeldså, J., Christidis, L., and Ericson, P.G. (2009). An unexpectedly long history of sexual selection in birds-of-paradise. BMC evolutionary biology *9*, 235.
8. Irestedt, M., Batalha-Filho, H., Ericson, P.G., Christidis, L., and Schodde, R. (2017). Phylogeny, biogeography and taxonomic consequences in a bird-of-paradise species complex, Lophorina–Ptiloris (Aves: Paradisaeidae). Zoological Journal of the Linnean Society *181*, 439-470.
9. Scholes, E., and Laman, T.G. (2018). Distinctive courtship phenotype of the Vogelkop Superb Bird-of-Paradise Lophorina niedda Mayr, 1930 confirms new species status. PeerJ *6*, e4621.
10. Bi, K., Linderoth, T., Vanderpool, D., Good, J.M., Nielsen, R., and Moritz, C. (2013). Unlocking the vault: next□generation museum population genomics. Molecular Ecology *22*, 6018-6032.
11. Poelstra, J.W., Vijay, N., Bossu, C.M., Lantz, H., Ryll, B., Müller, I., Baglione, V., Unneberg, P., Wikelski, M., and Grabherr, M.G. (2014). The genomic landscape underlying phenotypic integrity in the face of gene flow in crows. Science *344*, 1410-1414.
12. Zhan, X., Pan, S., Wang, J., Dixon, A., He, J., Muller, M.G., Ni, P., Hu, L., Liu, Y., and Hou, H. (2013). Peregrine and saker falcon genome sequences provide insights into evolution of a predatory lifestyle. Nature genetics *45*, 563.
13. Zhang, G., Li, C., Li, Q., Li, B., Larkin, D.M., Lee, C., Storz, J.F., Antunes, A., Greenwold, M.J., and Meredith, R.W. (2014). Comparative genomics reveals insights into avian genome evolution and adaptation. Science *346*, 1311-1320.
14. Burga, A., Wang, W., Ben-David, E., Wolf, P.C., Ramey, A.M., Verdugo, C., Lyons, K., Parker, P.G., and Kruglyak, L. (2017). A genetic signature of the evolution of loss of flight in the Galapagos cormorant. Science *356*, eaal3345.
15. Simão, F.A., Waterhouse, R.M., Ioannidis, P., Kriventseva, E.V., and Zdobnov, E.M. (2015). BUSCO: assessing genome assembly and annotation completeness with single-copy orthologs. Bioinformatics *31*, 3210-3212.
16. Kapusta, A., and Suh, A. (2017). Evolution of bird genomes—a transposon's□eye view. Annals of the New York Academy of Sciences *1389*, 164-185.
17. Suh, A., Bachg, S., Donnellan, S., Joseph, L., Brosius, J., Kriegs, J.O., and Schmitz, J. (2017). De-novo emergence of SINE retroposons during the early evolution of passerine birds. Mobile DNA *8*, 21.

18. Hillier, L., Miller, W., Birney, E., Warren, W., Hardison, R., Ponting, C., Bork, P., Burt, D., Groenen, M., and Delany, M. (2004). International Chicken Genome Sequencing Consortium: Sequence and comparative analysis of the chicken genome provide unique perspectives on vertebrate evolution. Nature *432*, 69-716.
19. Suh, A. (2016). The phylogenomic forest of bird trees contains a hard polytomy at the root of Neoaves. Zoologica Scripta *45*, 50-62.
20. Jarvis, E.D., Mirarab, S., Aberer, A.J., Li, B., Houde, P., Li, C., Ho, S.Y., Faircloth, B.C., Nabholz, B., and Howard, J.T. (2014). Whole-genome analyses resolve early branches in the tree of life of modern birds. Science *346*, 1320-1331.
21. Prum, R.O., Berv, J.S., Dornburg, A., Field, D.J., Townsend, J.P., Lemmon, E.M., and Lemmon, A.R. (2015). A comprehensive phylogeny of birds (Aves) using targeted next-generation DNA sequencing. Nature *526*, 569.
22. Murrell, B., Weaver, S., Smith, M.D., Wertheim, J.O., Murrell, S., Aylward, A., Eren, K., Pollner, T., Martin, D.P., and Smith, D.M. (2015). Gene-wide identification of episodic selection. Molecular Biology and Evolution *32*, 1365-1371.
23. De Bie, T., Cristianini, N., Demuth, J.P., and Hahn, M.W. (2006). CAFE: a computational tool for the study of gene family evolution. Bioinformatics *22*, 1269-1271.
24. Ellegren, H. (2010). Evolutionary stasis: the stable chromosomes of birds. Trends in Ecology & Evolution *25*, 283-291.
25. Lieberman-Aiden, E., Van Berkum, N.L., Williams, L., Imakaev, M., Ragoczy, T., Telling, A., Amit, I., Lajoie, B.R., Sabo, P.J., and Dorschner, M.O. (2009). Comprehensive mapping of long-range interactions reveals folding principles of the human genome. Science *326*, 289-293.
26. Maddison, W.P., and Knowles, L.L. (2006). Inferring phylogeny despite incomplete lineage sorting. Systematic biology *55*, 21-30.
27. Suh, A., Smeds, L., and Ellegren, H. (2015). The dynamics of incomplete lineage sorting across the ancient adaptive radiation of neoavian birds. PLoS biology *13*, e1002224.
28. Feschotte, C. (2008). Transposable elements and the evolution of regulatory networks. Nature Reviews Genetics *9*, 397.
29. Oliver, K.R., and Greene, W.K. (2009). Transposable elements: powerful facilitators of evolution. Bioessays *31*, 703-714.
30. Lowe, C.B., Kellis, M., Siepel, A., Raney, B.J., Clamp, M., Salama, S.R., Kingsley, D.M., Lindblad-Toh, K., and Haussler, D. (2011). Three periods of regulatory innovation during vertebrate evolution. Science *333*, 1019-1024.
31. Jurka, J., Bao, W., and Kojima, K.K. (2011). Families of transposable elements, population structure and the origin of species. Biology Direct *6*, 44.
32. Fox, H.M., and Ververs, G. (1960). The Nature of Animal Colors., (New York: MacMillan).
33. Fox, D.L. (1976). Animal biochromes and structural colours: physical, chemical, distributional & physiological features of coloured bodies in the animal world, (Univ of California Press).
34. Zi, J., Yu, X., Li, Y., Hu, X., Xu, C., Wang, X., Liu, X., and Fu, R. (2003). Coloration strategies in peacock feathers. Proceedings of the National Academy of Sciences *100*, 12576-12578.
35. Wilts, B.D., Michielsen, K., De Raedt, H., and Stavenga, D.G. (2014). Sparkling feather reflections of a bird-of-paradise explained by finite-difference time-domain modeling. Proceedings of the National Academy of Sciences *111*, 4363-4368.
36. Stavenga, D.G., Leertouwer, H.L., Marshall, N.J., and Osorio, D. (2010). Dramatic colour changes in a bird of paradise caused by uniquely structured breast feather barbules. Proceedings of the Royal Society of London B: Biological Sciences, rspb20102293.

37. Dale, J., Dey, C.J., Delhey, K., Kempenaers, B., and Valcu, M. (2015). The effects of life history and sexual selection on male and female plumage colouration. Nature *527*, 367.
38. Silver, D.L., Hou, L., Somerville, R., Young, M.E., Apte, S.S., and Pavan, W.J. (2008). The secreted metalloprotease ADAMTS20 is required for melanoblast survival. PLoS genetics *4*, e1000003.
39. Bennett, D.C., and Lamoreux, M.L. (2003). The color loci of mice–a genetic century. Pigment Cell & Melanoma Research *16*, 333-344.
40. Noji, S., Koyama, E., Myokai, F., Nohno, T., Ohuchi, H., Nishikawa, K., and Taniguchi, S. (1993). Differential expression of three chick FGF receptor genes, FGFR1, FGFR2 and FGFR3, in limb and feather development. Progress in clinical and biological research *383*, 645-654.
41. Gfrerer, L., Shubinets, V., Hoyos, T., Kong, Y., Nguyen, C., Pietschmann, P., Morton, C.C., Maas, R.L., and Liao, E.C. (2014). Functional analysis of SPECC1L in craniofacial development and oblique facial cleft pathogenesis. Plastic and reconstructive surgery *134*, 748.
42. Wada, T., Nakashima, T., Oliveira-dos-Santos, A.J., Gasser, J., Hara, H., Schett, G., and Penninger, J.M. (2005). The molecular scaffold Gab2 is a crucial component of RANK signaling and osteoclastogenesis. Nature medicine *11*, 394.
43. Stelzer, C., Brimmer, A., Hermanns, P., Zabel, B., and Dietz, U.H. (2007). Expression profile of Papss2 (3′□phosphoadenosine 5′□phosphosulfate synthase 2) during cartilage formation and skeletal development in the mouse embryo. Developmental Dynamics *236*, 1313-1318.
44. Kukita, T., Wada, N., Kukita, A., Kakimoto, T., Sandra, F., Toh, K., Nagata, K., Iijima, T., Horiuchi, M., and Matsusaki, H. (2004). RANKL-induced DC-STAMP is essential for osteoclastogenesis. Journal of Experimental Medicine *200*, 941-946.
45. van der Valk, R.J., Kreiner-Møller, E., Kooijman, M.N., Guxens, M., Stergiakouli, E., Sääf, A., Bradfield, J.P., Geller, F., Hayes, M.G., and Cousminer, D.L. (2014). A novel common variant in DCST2 is associated with length in early life and height in adulthood. Human molecular genetics *24*, 1155-1168.
46. Delfini, M., Hirsinger, E., Pourquié, O., and Duprez, D. (2000). Delta 1-activated notch inhibits muscle differentiation without affecting Myf5 and Pax3 expression in chick limb myogenesis. Development *127*, 5213-5224.
47. Li, J., Zhao, X.-L., Gilbert, E.R., Li, D.-Y., Liu, Y.-P., Wang, Y., Zhu, Q., Wang, Y.-G., Chen, Y., and Tian, K. (2014). APOBEC2 mRNA and protein is predominantly expressed in skeletal and cardiac muscles of chickens. Gene *539*, 263-269.
48. Harris, R.S., Bishop, K.N., Sheehy, A.M., Craig, H.M., Petersen-Mahrt, S.K., Watt, I.N., Neuberger, M.S., and Malim, M.H. (2003). DNA deamination mediates innate immunity to retroviral infection. Cell *113*, 803-809.
49. Mangeat, B., Turelli, P., Caron, G., Friedli, M., Perrin, L., and Trono, D. (2003). Broad antiretroviral defence by human APOBEC3G through lethal editing of nascent reverse transcripts. Nature *424*, 99.
50. Knisbacher, B.A., and Levanon, E.Y. (2015). DNA editing of LTR retrotransposons reveals the impact of APOBECs on vertebrate genomes. Molecular Biology and Evolution *33*, 554-567.
51. Haeseleer, F., Imanishi, Y., Maeda, T., Possin, D.E., Maeda, A., Lee, A., Rieke, F., and Palczewski, K. (2004). Essential role of Ca 2+-binding protein 4, a Ca v 1.4 channel regulator, in photoreceptor synaptic function. Nature neuroscience *7*, 1079.
52. Kobayashi, M., Hara, K., Ruth, T.Y., and Yasuda, K. (2008). Expression and functional analysis of Nr2e3, a photoreceptor-specific nuclear receptor, suggest common mechanisms in retinal development between avians and mammals. Development genes and evolution *218*, 439-444.

53. Swiderski, R.E., Ross, J.L., Fingert, J.H., Clark, A.F., Alward, W.L., Stone, E.M., and Sheffield, V.C. (2000). Localization of MYOC transcripts in human eye and optic nerve by in situ hybridization. Investigative ophthalmology & visual science *41*, 3420-3428.
54. Lind, O., Henze, M.J., Kelber, A., and Osorio, D. (2017). Coevolution of coloration and colour vision? Phil. Trans. R. Soc. B *372*, 20160338.
55. Price, T.D. (2017). Sensory drive, color, and color vision. The American Naturalist *190*, 157-170.
56. Mundy, N.I., Stapley, J., Bennison, C., Tucker, R., Twyman, H., Kim, K.-W., Burke, T., Birkhead, T.R., Andersson, S., and Slate, J. (2016). Red carotenoid coloration in the zebra finch is controlled by a cytochrome P450 gene cluster. Current Biology *26*, 1435-1440.
57. Bloch, N.I. (2015). Evolution of opsin expression in birds driven by sexual selection and habitat. Proceedings of the Royal Society of London B: Biological Sciences *282*, 20142321.
58. Bowers, J.M., and Alexander, B.K. (1967). Mice: individual recognition by olfactory cues. Science *158*, 1208-1210.
59. Ables, E.M., Kay, L.M., and Mateo, J.M. (2007). Rats assess degree of relatedness from human odors. Physiology & behavior *90*, 726-732.
60. Smith, T.E., Tomlinson, A.J., Mlotkiewicz, J.A., and Abbott, D.H. (2001). Female marmoset monkeys (Callithrix jacchus) can be identified from the chemical composition of their scent marks. Chemical senses *26*, 449-458.
61. Johansson, B.G., and Jones, T.M. (2007). The role of chemical communication in mate choice. Biological Reviews *82*, 265-289.
62. Roper, T.J. (1999). Olfaction in birds. Advances in the Study of Behavior *28*, 247-247.
63. Khan, I., Yang, Z., Maldonado, E., Li, C., Zhang, G., Gilbert, M.T.P., Jarvis, E.D., O'Brien, S.J., Johnson, W.E., and Antunes, A. (2015). Olfactory receptor subgenomes linked with broad ecological adaptations in Sauropsida. Molecular Biology and Evolution *32*, 2832-2843.
64. Yokosuka, M., Hagiwara, A., Saito, T.R., Tsukahara, N., Aoyama, M., Wakabayashi, Y., Sugita, S., and Ichikawa, M. (2009). Histological properties of the nasal cavity and olfactory bulb of the Japanese jungle crow Corvus macrorhynchos. Chemical senses *34*, 581-593.
65. Retzek, H., Steyrer, E., Sanders, E., Nimpf, J., and Schneider, W. (1992). Molecular cloning and functional characterization of chicken cathepsin D, a key enzyme for yolk formation. DNA and cell biology *11*, 661-672.
66. Bourin, M., Gautron, J., Berges, M., Nys, Y., and Réhault-Godbert, S. (2012). Sex-and tissue-specific expression of "similar to nothepsin" and cathepsin D in relation to egg yolk formation in Gallus gallus. Poultry science *91*, 2288-2293.
67. Biason-Lauber, A., Konrad, D., Meyer, M., and Schoenle, E.J. (2009). Ovaries and female phenotype in a girl with 46, XY karyotype and mutations in the CBX2 gene. The American Journal of Human Genetics *84*, 658-663.
68. Koopman, P., Gubbay, J., Vivian, N., Goodfellow, P., and Lovell-Badge, R. (1991). Male development of chromosomally female mice transgenic for Sry. Nature *351*, 117.
69. Nagarkatti-Gude, D.R., Jaimez, R., Henderson, S.C., Teves, M.E., Zhang, Z., and Strauss III, J.F. (2011). Spag16, an axonemal central apparatus gene, encodes a male germ cell nuclear speckle protein that regulates SPAG16 mRNA expression. PLoS one *6*, e20625.
70. Lovasco, L.A., Seymour, K.A., Zafra, K., O'Brien, C.W., Schorl, C., and Freiman, R.N. (2010). Accelerated ovarian aging in the absence of the transcription regulator TAF4B in mice. Biology of reproduction *82*, 23-34.

71. Tazawa, S., Yamato, T., Fujikura, H., Hiratochi, M., Itoh, F., Tomae, M., Takemura, Y., Maruyama, H., Sugiyama, T., and Wakamatsu, A. (2005). SLC5A9/SGLT4, a new Na+-dependent glucose transporter, is an essential transporter for mannose, 1, 5-anhydro-D-glucitol, and fructose. Life sciences *76*, 1039-1050.
72. Foster, J.D., Pederson, B.A., and Nordlie, R.C. (1997). Glucose-6-phosphatase structure, regulation, and function: an update. Proceedings of the Society for Experimental Biology and Medicine *215*, 314-332.
73. Mirsky, I., and Broh-Kahn, R. (1949). The inactivation of insulin by tissue extracts; the distribution and properties of insulin inactivating extracts. Archives of biochemistry *20*, 1.
74. Sweazea, K.L., McMurtry, J.P., and Braun, E.J. (2006). Inhibition of lipolysis does not affect insulin sensitivity to glucose uptake in the mourning dove. Comparative Biochemistry and Physiology Part B: Biochemistry and Molecular Biology *144*, 387-394.
75. Danby, R., Martin, I., and Gibson, W. (1982). Effects of pancreatectomy, tolbutamide and insulin on glucose fluxes in chickens. Journal of Endocrinology *94*, 429-441.
76. Gayathri, K., Shenoy, K., and Hegde, S. (2004). Blood profile of pigeons (Columba livia) during growth and breeding. Comparative Biochemistry and Physiology Part A: Molecular & Integrative Physiology *138*, 187-192.
77. Holmes, D., Flückiger, R., and Austad, S. (2001). Comparative biology of aging in birds: an update. Experimental gerontology *36*, 869-883.
78. Ku, H.-H., and Sohal, R. (1993). Comparison of mitochondrial pro-oxidant generation and anti-oxidant defenses between rat and pigeon: possible basis of variation in longevity and metabolic potential. Mechanisms of ageing and development *72*, 67-76.
79. Castillo, C.G., Lo, W., Kuck, J., and Yu, N.T. (1992). Nature and localization of avian lens glycogen by electron microscopy and Raman spectroscopy. Biophysical journal *61*, 839-844.
80. Irestedt, M., Ohlson, J.I., Zuccon, D., Källersjö, M., and Ericson, P.G. (2006). Nuclear DNA from old collections of avian study skins reveals the evolutionary history of the Old World suboscines (Aves, Passeriformes). Zoologica Scripta *35*, 567-580.
81. Meyer, M., and Kircher, M. (2010). Illumina sequencing library preparation for highly multiplexed target capture and sequencing. Cold Spring Harbor Protocols *2010*, pdb. prot5448.
82. Andrews, S. (2010). FASTQC. A quality control tool for high throughput sequence data. URL http://www.bioinformatics.babraham.ac.uk/projects/fastqc.
83. Simpson, J.T. (2013). Exploring Genome Characteristics and Sequence Quality Without a Reference. arXiv preprint arXiv:1307.8026.
84. Simpson, J.T., and Durbin, R. (2012). Efficient de novo assembly of large genomes using compressed data structures. Genome Research *22*, 549-556.
85. Gnerre, S., MacCallum, I., Przybylski, D., Ribeiro, F.J., Burton, J.N., Walker, B.J., Sharpe, T., Hall, G., Shea, T.P., and Sykes, S. (2011). High-quality draft assemblies of mammalian genomes from massively parallel sequence data. Proceedings of the National Academy of Sciences *108*, 1513-1518.
86. Luo, R., Liu, B., Xie, Y., Li, Z., Huang, W., Yuan, J., He, G., Chen, Y., Pan, Q., and Liu, Y. (2012). SOAPdenovo2: an empirically improved memory-efficient short-read de novo assembler. GigaScience *1*, 18.
87. Parra, G., Bradnam, K., and Korf, I. (2007). CEGMA: a pipeline to accurately annotate core genes in eukaryotic genomes. Bioinformatics *23*, 1061-1067.
88. Li, H., and Durbin, R. (2009). Fast and accurate short read alignment with Burrows–Wheeler transform. Bioinformatics *25*, 1754-1760.
89. Li, H., Handsaker, B., Wysoker, A., Fennell, T., Ruan, J., Homer, N., Marth, G., Abecasis, G., and Durbin, R. (2009). The sequence alignment/map format and SAMtools. Bioinformatics *25*, 2078-2079.

90. McKenna, A., Hanna, M., Banks, E., Sivachenko, A., Cibulskis, K., Kernytsky, A., Garimella, K., Altshuler, D., Gabriel, S., and Daly, M. (2010). The Genome Analysis Toolkit: a MapReduce framework for analyzing next-generation DNA sequencing data. Genome Research *20*, 1297-1303.
91. Korneliussen, T.S., Albrechtsen, A., and Nielsen, R. (2014). ANGSD: analysis of next generation sequencing data. BMC bioinformatics *15*, 356.
92. Smit, A., Hubley, R., and Green, P. (2014). RepeatModeler Open-1.0. 2008-2010.
93. Bao, Z., and Eddy, S.R. (2002). Automated de novo identification of repeat sequence families in sequenced genomes. Genome Research *12*, 1269-1276.
94. Price, A.L., Jones, N.C., and Pevzner, P.A. (2005). De novo identification of repeat families in large genomes. Bioinformatics *21*, i351-i358.
95. Benson, G. (1999). Tandem repeats finder: a program to analyze DNA sequences. Nucleic Acids Research *27*, 573.
96. Jurka, J., Kapitonov, V.V., Pavlicek, A., Klonowski, P., Kohany, O., and Walichiewicz, J. (2005). Repbase Update, a database of eukaryotic repetitive elements. Cytogenetic and genome research *110*, 462-467.
97. Smeds, L., Warmuth, V., Bolivar, P., Uebbing, S., Burri, R., Suh, A., Nater, A., Bureš, S., Garamszegi, L.Z., and Hogner, S. (2015). Evolutionary analysis of the female-specific avian W chromosome. Nature communications *6*, 7330.
98. Suh, A., Smeds, L., and Ellegren, H. (2018). Abundant recent activity of retrovirus□like retrotransposons within and among flycatcher species implies a rich source of structural variation in songbird genomes. Molecular Ecology *27*, 99-111.
99. Vijay, N., Bossu, C.M., Poelstra, J.W., Weissensteiner, M.H., Suh, A., Kryukov, A.P., and Wolf, J.B. (2016). Evolution of heterogeneous genome differentiation across multiple contact zones in a crow species complex. Nature communications *7*, 13195.
100. Platt, R.N., Blanco-Berdugo, L., and Ray, D.A. (2016). Accurate transposable element annotation is vital when analyzing new genome assemblies. Genome biology and evolution *8*, 403-410.
101. Lavoie, C.A., Platt, R.N., Novick, P.A., Counterman, B.A., and Ray, D.A. (2013). Transposable element evolution in Heliconius suggests genome diversity within Lepidoptera. Mobile DNA *4*, 21.
102. Altschul, S.F., Madden, T.L., Schäffer, A.A., Zhang, J., Zhang, Z., Miller, W., and Lipman, D.J. (1997). Gapped BLAST and PSI-BLAST: a new generation of protein database search programs. Nucleic Acids Research *25*, 3389-3402.
103. Katoh, K., and Standley, D.M. (2013). MAFFT multiple sequence alignment software version 7: improvements in performance and usability. Molecular Biology and Evolution *30*, 772-780.
104. Smit, A., Hubley, R., and Green, P. 1996–2010. RepeatMasker Open-3.0.
105. Grabherr, M.G., Russell, P., Meyer, M., Mauceli, E., Alföldi, J., Di Palma, F., and Lindblad-Toh, K. (2010). Genome-wide synteny through highly sensitive sequence alignment: Satsuma. Bioinformatics *26*, 1145-1151.
106. Krzywinski, M., Schein, J., Birol, I., Connors, J., Gascoyne, R., Horsman, D., Jones, S.J., and Marra, M.A. (2009). Circos: an information aesthetic for comparative genomics. Genome Research *19*, 1639-1645.
107. Holt, C., and Yandell, M. (2011). MAKER2: an annotation pipeline and genome-database management tool for second-generation genome projects. BMC bioinformatics *12*, 491.
108. Korf, I. (2004). Gene finding in novel genomes. BMC bioinformatics *5*, 59.
109. Stanke, M., and Waack, S. (2003). Gene prediction with a hidden Markov model and a new intron submodel. Bioinformatics *19*, ii215-ii225.

110. Lechner, M., Hernandez-Rosales, M., Doerr, D., Wieseke, N., Thévenin, A., Stoye, J., Hartmann, R.K., Prohaska, S.J., and Stadler, P.F. (2014). Orthology detection combining clustering and synteny for very large datasets. PLoS one *9*, e105015.
111. Löytynoja, A., and Goldman, N. (2005). An algorithm for progressive multiple alignment of sequences with insertions. Proceedings of the National Academy of Sciences of the United States of America *102*, 10557-10562.
112. Kück, P., Meusemann, K., Dambach, J., Thormann, B., von Reumont, B.M., Wägele, J.W., and Misof, B. (2010). Parametric and non-parametric masking of randomness in sequence alignments can be improved and leads to better resolved trees. Frontiers in zoology *7*, 1.
113. Kück, P. (2009). ALICUT: a Perlscript which cuts ALISCORE identified RSS. Department of Bioinformatics, Zoologisches Forschungsmuseum A. Koenig (ZFMK), Bonn, Germany, version *2*.
114. Stamatakis, A. (2014). RAxML version 8: a tool for phylogenetic analysis and post-analysis of large phylogenies. Bioinformatics, btu033.
115. Mirarab, S., Bayzid, M.S., Boussau, B., and Warnow, T. (2014). Statistical binning enables an accurate coalescent-based estimation of the avian tree. Science *346*, 1250463.
116. Mirarab, S., Reaz, R., Bayzid, M.S., Zimmermann, T., Swenson, M.S., and Warnow, T. (2014). ASTRAL: genome-scale coalescent-based species tree estimation. Bioinformatics *30*, i541-i548.
117. Kozlov, A.M., Aberer, A.J., and Stamatakis, A. (2015). ExaML version 3: a tool for phylogenomic analyses on supercomputers. Bioinformatics *31*, 2577-2579.
118. Sanderson, M.J. (2003). r8s: inferring absolute rates of molecular evolution and divergence times in the absence of a molecular clock. Bioinformatics *19*, 301-302.
119. Yang, Z. (2007). PAML 4: phylogenetic analysis by maximum likelihood. Molecular Biology and Evolution *24*, 1586-1591.
120. Pond, S.L.K., and Muse, S.V. (2005). HyPhy: hypothesis testing using phylogenies. In Statistical methods in molecular evolution. (Springer), pp. 125-181.
121. Mudunuri, U., Che, A., Yi, M., and Stephens, R.M. (2009). bioDBnet: the biological database network. Bioinformatics *25*, 555-556.
122. Zerbino, D.R., Achuthan, P., Akanni, W., Amode, M.R., Barrell, D., Bhai, J., Billis, K., Cummins, C., Gall, A., and Girón, C.G. (2017). Ensembl 2018. Nucleic Acids Research *46*, D754-D761.
123. Enright, A.J., Van Dongen, S., and Ouzounis, C.A. (2002). An efficient algorithm for large-scale detection of protein families. Nucleic Acids Research *30*, 1575-1584.
124. Hedges, S.B., Dudley, J., and Kumar, S. (2006). TimeTree: a public knowledge-base of divergence times among organisms. Bioinformatics *22*, 2971-2972.
125. Han, M.V., Thomas, G.W., Lugo-Martinez, J., and Hahn, M.W. (2013). Estimating gene gain and loss rates in the presence of error in genome assembly and annotation using CAFE 3. Molecular Biology and Evolution *30*, 1987-1997.

Supplementary

Supplementary Figures

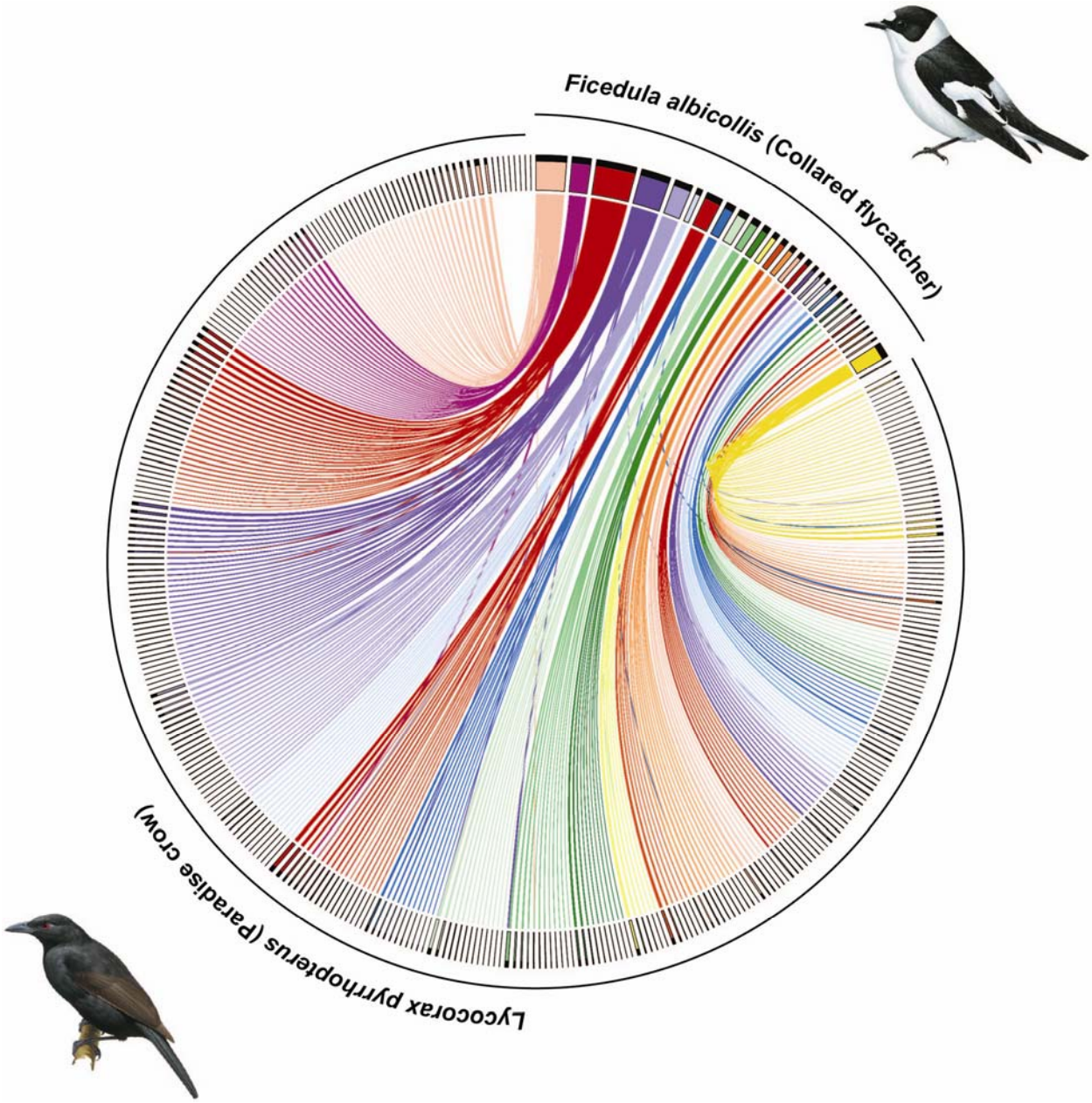

Supplementary Figure S1: Chromosomal synteny plot between the collared flycatcher and the Paradise crow. The plot shows scaffolds bigger than 50kb and links (alignments) bigger than 2kb.

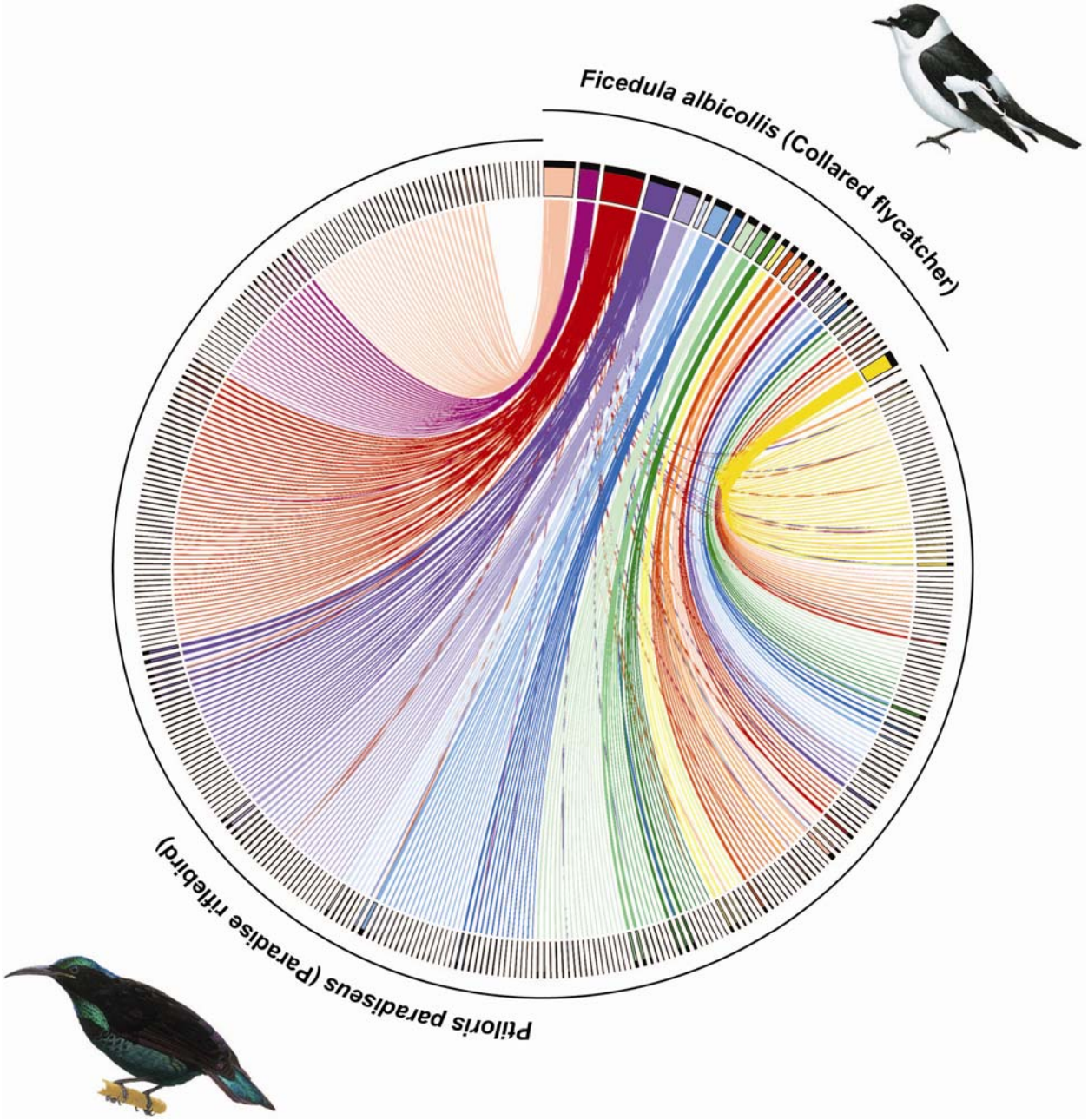

Supplementary Figure S2: Chromosomal synteny plot between the collared flycatcher and the Paradise riflebird. The plot shows scaffolds bigger than 50kb and links (alignments) bigger than 2kb.

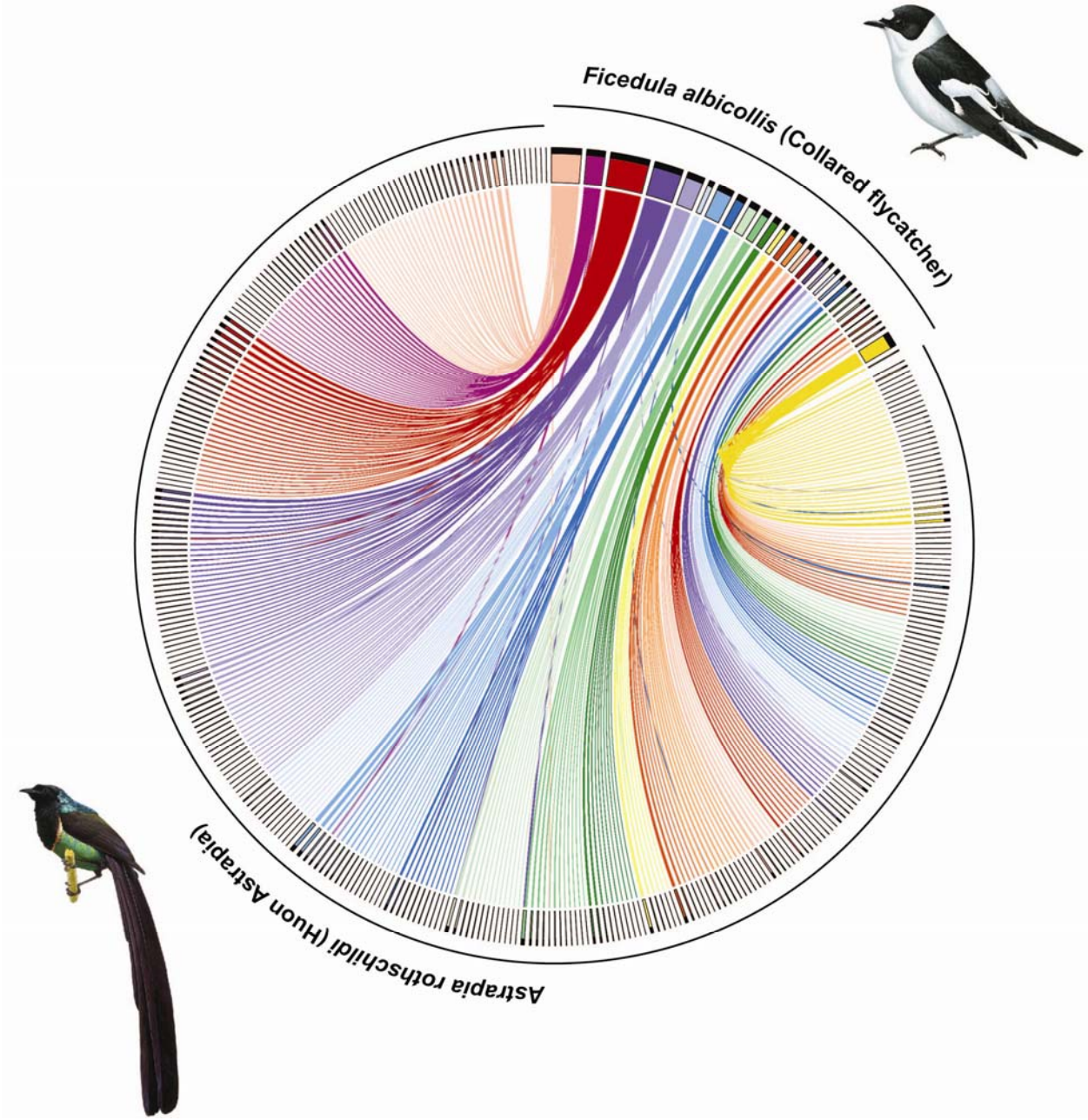

Supplementary Figure S3: Chromosomal synteny plot between the collared flycatcher and the Huon Astrapia. The plot shows scaffolds bigger than 50kb and links (alignments) bigger than 2kb.

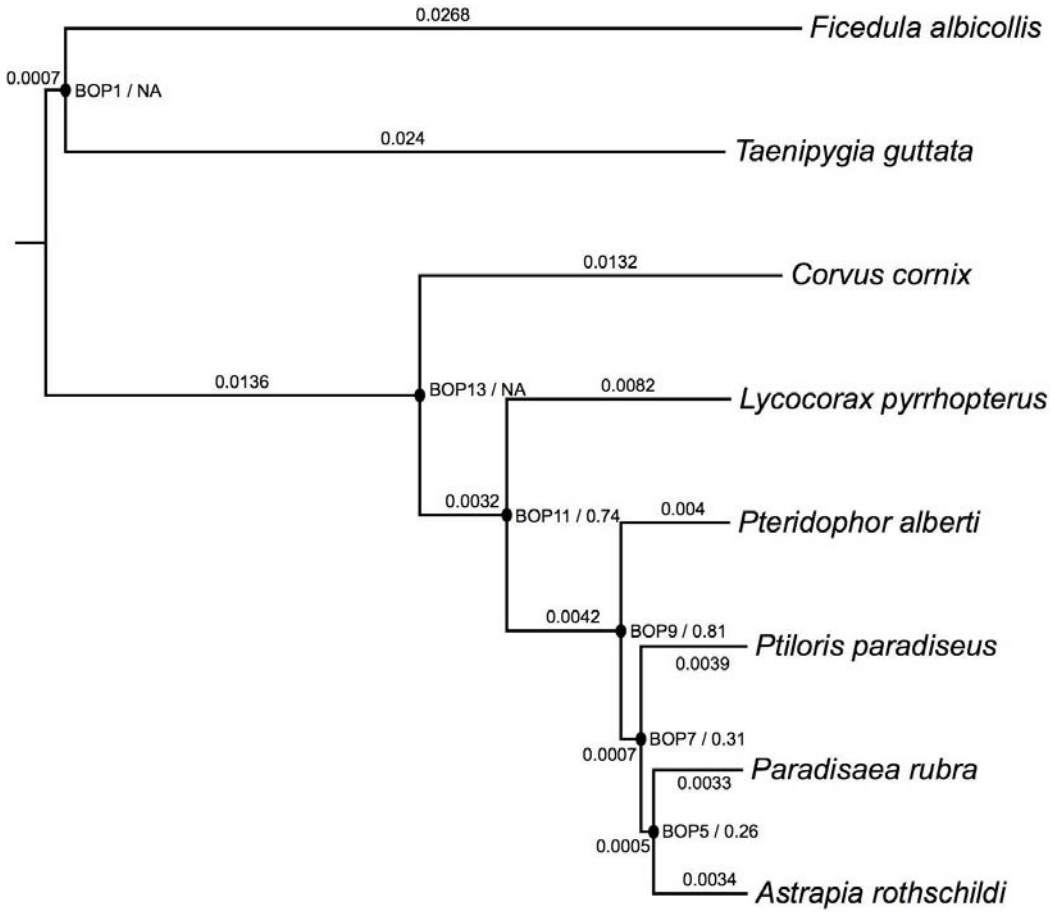

Supplementary Figure S4: Phylogenetic species tree. The species tree was reconstructed from individual maximum likelihood-based gene trees using 4,656 exons and coalescent-based statistical binning (Astral). Branch lengths are depicted on the branches (calculated via a ML tree constructed using ExaML and 200 randomly selected genes). Nodes are labelled and concordance factor is shown next to the node labels (ie [node label] / [concordance factor]). All nodes have 100 bootstrap support.

Supplementary Tables

Supplementary Table S1: *De novo* Assembly Statistics.

	# Contigs	**Scaffold N50**	**Assembly Length**
Astrapia rothschildi	2,081	7.7Mb	1.03Gb
Lycocorax pyrrhopterus	3,216	4.2Mb	1.07Gb
Ptiloris paradiseus	2,062	4.27Mb	1.04Gb

Supplementary Table S2: BUSCO scores. Scores were calculated using Busco2 and the aves_odb9 data set (4,915 genes total).

	Complete	**Duplicated**	**Fragmented**	**Missing**
Astrapia rothschildi	4,669 (95.0%)	48 (1.0%)	139 (2.8%)	107 (2.2%)
Lycocorax pyrrhopterus	4,659 (93.8%)	51 (1.0%)	161 (3.3%)	95 (1.9%)
Ptiloris paradiseus	4,675 (95.1%)	44 (0.9%)	135 (2.7%)	105 (2.2%)
Paradisaea rubra	4,662 (94.9%)	47 (1.0%)	150 (3.1%)	103 (2.0%)
Pteridophor alberti	4,661 (94.8%)	39 (0.8%)	155 (3.2%)	99 (2.0%)

Supplementary Table S3: Annotation.

	# of Transcripts	Average transcript size (bp)	Average introns size (kb)	Average # of introns per gene
Astrapia rothschildi	16,260	1,603	2.2	9
Lycocorax pyrrhopterus	17,023	1,572	2.2	9
Ptiloris paradiseus	17,269	1,584	2.2	9
Paradisaea rubra	16,822	1,561	2.2	9
Pteridophor alberti	16,721	1,562	2.2	9

Supplementary Table S4: RepeatMasker annotation of the three birds-of-paradise genome assemblies using a library of our *de novo* repeat annotations of birds-of-paradise merged with existing avian repeat libraries.

	Astrapia rothschildi			*Lycocorax pyrrhopterus*			*Ptiloris paradisaeus*		
Repeat type	**Copies**	**Total bp**	**Total %**	**Copies**	**Total bp**	**Total %**	**Copies**	**Total bp**	**Total %**
SINE	8,019	966,992	0.09	7,974	955,190	0.09	7,977	961,945	0.09
LINE	128,473	38,885,201	3.67	130,706	40,271,136	3.76	129,094	38,994,767	3.68
LTR	38,693	20,692,445	1.95	48,395	27,819,221	2.60	39,123	21,311,765	2.01
DNA	4,582	790,017	0.07	4,734	845,120	0.08	4,617	790,421	0.07
Unclassified	34,049	9,005,494	0.85	37,519	9,167,482	0.86	30,814	8,931,323	0.84
Total interspersed repeats	**213,816**	**70,340,149**	**6.63**	**229,328**	**79,058,149**	**7.39**	**211,625**	**70,990,221**	**6.69**
Small RNA	538	46,523	0.00	577	50,738	0.00	546	47,744	0.00
Satellites	2,884	623,756	0.06	2,706	572,161	0.05	2,855	646,354	0.06
Simple repeats	195,600	9,348,199	0.88	193,765	9,101,884	0.85	197,648	9,318,098	0.88
Low complexity	43,076	2,388,544	0.23	42,067	2,292,784	0.21	42,546	2,360,570	0.22
Total tandem repeats	242,098	12,407,022	1.17	239,115	12,017,567	1.11	243,595	12,372,766	1.16
Total repeats	455,914	82,747,171	7.80	468,443	91,075,716	8.50	455,220	83,362,987	7.85
Assembly		1.06Gb			1.07Gb			1.06Gb	
Gap ('N') bp		13,196,877			10,466,138			10,993,394	

Supplementary Table S5: Characteristics of the manually curated TE consensus sequences from *Lycocorax pyrrhopterus*, including lineage-specific LTR families termed as 'lycPyrLTR*'.

Class	Subclass	Superfamily	Family	Subfamily	Similarity to known repeats	Consensus status	Consensus length	TSD
Retrotransposon	LTR	ERV1	lycPyrLTR1	lycPyrLTR1	None	Complete	463	4 bp
Retrotransposon	LTR	ERV1	lycPyrLTR2	lycPyrLTR2	None	Complete	535	4 bp
Retrotransposon	LTR	ERV1	lycPyrLTR3	lycPyrLTR3	None	Complete	623	4 bp
Retrotransposon	LTR	ERV1	TguERV3	TguERV3_LTR2b-L_lycPyr	Partially TguERV3_LTR2b (68% similarity)	Complete	601	4 bp
Retrotransposon	LTR	ERV1	TguERV1	TguERV1_LTR1a-L_lycPyr	Partially TguERV1_LTR1a (72% similarity)	Complete	600	4 bp
Retrotransposon	LTR	ERV1	TguLTR11	TguLTR11l-L_lycPyr.inc	Partially TguLTR11l + TguERV2_I + TguERV1_I + TguERV3_I (79% + 65% + 63% + 66% similarity)	Incomplete 3' end	4535	?
Retrotransposon	LTR	ERV1	TguLTR12	TguLTR12-L_lycPyr.inc	Partially TguLTR12 (84% similarity)	Incomplete TSD	625	?
Retrotransposon	LTR	ERV2	lycPyrLTRK1	lycPyrLTRK1a	None	Complete	366	6 bp
Retrotransposon	LTR	ERV2	lycPyrLTRK1	lycPyrLTRK1b	None	Complete	366	6 bp
Retrotransposon	LTR	ERV2	lycPyrLTRK2	lycPyrLTRK2	None	Complete	647	6 bp
Retrotransposon	LTR	ERV2	lycPyrLTRK3	lycPyrLTRK3a	None	Complete	689	6 bp
Retrotransposon	LTR	ERV2	lycPyrLTRK3	lycPyrLTRK3b	None	Complete	744	6 bp
Retrotransposon	LTR	ERV2	lycPyrLTRK4	lycPyrLTRK4	None	Complete	605	6 bp

Retrotransposon	LTR	ERV2	lycPyrLTRK5	lycPyrLTRK5	None	Com-plete	397	6 bp
Retrotransposon	LTR	ERV2	lycPyrLTRK6	lycPyrLTRK6	None	Com-plete	666	6 bp
Retrotransposon	LTR	ERV2	lycPyrLTRK7	lycPyrLTRK7	None	Com-plete	334	6 bp
Retrotransposon	LTR	ERV2	lycPyrLTRK8	lycPyrLTRK8	None	Com-plete	408	6 bp
Retrotransposon	LTR	ERV2	lycPyrLTRK9	lycPyrLTRK9_LTR	None	Com-plete	380	6 bp
Retrotransposon	LTR	ERV2	lycPyrLTRK9	lycPyrLTRK9_I.inc	None	Incom-plete 3' end	537	6 bp
Retrotransposon	LTR	ERV3	lycPyrLTRL1	lycPyrLTRL1	None	Com-plete	1171	5 bp
Retrotransposon	LTR	ERV3	lycPyrLTRL2	lycPyrLTRL2	None	Com-plete	1105	5 bp
Retrotransposon	LTR	ERV3	lycPyrLTRL3	lycPyrLTRL3	None	Com-plete	460	5 bp
Retrotransposon	LTR	ERV3	lycPyrLTRL4	lycPyrLTRL4	None	Com-plete	807	5 bp
Retrotransposon	LTR	ERV3	lycPyrLTRL5	lycPyrLTRL5	None	Com-plete	1281	5 bp
Retrotransposon	LTR	ERV3	lycPyrLTRL6	lycPyrLTRL6	None	Com-plete	670	5 bp
Retrotransposon	LTR	ERV3	lycPyrLTRL7	lycPyrLTRL7.inc	Partially Tgu_rep3 (80% similarity)	Incom-plete 3' end	177	?
Retrotransposon	LTR	ERV3	TguERVL2	TguERVL2b-LTR-L_lycPyr	Partially TguERVL2b3_LTR + TguERVL2b1_LTR (85% + 79% similarity)	Com-plete	579	5 bp
Retrotransposon	LTR	ERV3	TguERVL2	TguERVL2a2-LTR-L_lycPyr	Partially TguERVL2a2-LTR (93% similarity)	Com-plete	941	5 bp
Retrotransposon	LTR	ERV3	TguLTRL1	TguLTRL1-La_lycPyr	Partially TguLTRL1a7 (75% similarity)	Com-plete	647	5 bp

Retrotransposon	LTR	ERV3	TguLTRL1	TguLTRL1-Lb_lycPyr.inc	Partially TguERVL1_I + TguLTRL1a6 + TguLTRL1a7 (88% + 77% + 74% similarity)	Incomplete 5' end	2729	?
Retrotransposon	LTR	ERV3	TguLTRL1	TguLTRL1-Lc_lycPyr.inc	Partially TguERVL1_I + TguERVL2_I + TguLTRL6b (80% + 78% + 97% similarity)	Incomplete 5' and 3' ends	1754	?
Retrotransposon	LTR	ERV3	TguLTRL1	TguLTRL1-Ld_lycPyr.inc	Partially TguLTRL1a6 + TguLTRL1a7 + TguLTRL1_I (77% + 75% + 75% similarity)	Incomplete 3' end	2655	?
Retrotransposon	LTR	ERV3	TguLTRL1	TguLTRL1-Le_lycPyr.inc	Partially TguLTRL1a7 + TguERVL1_I (75% + 77% similarity)	Incomplete 5' and 3' ends	3079	?
Unknown	Unknown	Unknown	Unknown	lycPyr5-275.3inc	None	Incomplete 3' end	177	?
Unknown	Unknown	Unknown	Unknown	lycPyr5-1942.inc	None	Incomplete 5' and 3' ends	620	?
Unknown	Unknown	Unknown	Unknown	lycPyr6-947.inc_sat	None	Incomplete 5' and 3' ends	3602	?

Supplementary Table S6: Top 10 gene tree topology counts (423 total topologies in 4,450 rooted gene trees). Average Robinson-Foulds distance for all 4,656 gene trees is 3.92. Z: Zebra finch; F: Collared Flycatcher; C: Crow; L: Lycocorax; Pte: Pteridophor; Pti: Ptiloris; Par: Paradisaea; A: Astrapia.

Topology	Count
((Z,F),(C,(L,(Pte,(Pti,(Par,A)))))	430
((Z,F),(C,(L,(Pte,((Pti,Par),A)))))	357
((Z,F),(C,(L,(Pte,(Par,(Pti,A)))))	279
((Z,F),(C,(L,(Pti,(Pte,(Par,A)))))	224
((Z,F),(C,(L,((Pti,Par),(Pte,A)))))	167
((Z,F),(C,(L,(Pti,((Pte,Par),A)))))	166
((Z,F),(C,(L,(((Pti,Par),Pte),A))))	162
((Z,F),(C,(L,((Pte,Pti),(Par,A)))))	161
((Z,F),(C,(L,((Pti,(Pte,Par)),A))))	159
((Z,F),(C,(L,(Pti,(Par,(Pte,A)))))	156

Supplementary Table S7: Saturation Analysis. Pairwise dn/ds ratio.

Astrapia							
Bilscor	0.036						
Ensfalt	0.046	0.063					
Enstgut	0.044	0.059	0.046				
Lycocorax	0.014	0.037	0.046	0.044			
Paradisaea	0.006	0.034	0.046	0.043	0.014		
Pteridophor	0.007	0.036	0.046	0.044	0.014	0.007	
Ptiloris	0.006	0.036	0.046	0.044	0.014	0.006	0.007

Supplementary Table S8. Genes under positive selection.

GenBank Accession	Gene Symbol
XM_016302299	RSPH14
XM_005060676	SNX18
XM_005061576	RSG1
XM_016299097	COL4A1
XM_016304880	MCTP1
XM_005042552	NDRG1
XM_005062657	MRPL34
XM_005057187	BPIFB2
XM_016298377	LOC101809528
XM_005057074	LOC101821424
XM_016301269	LOC101807976
XM_016302077	TRAFD1
XM_005048141	*SH2D4B*
XM_005044853	MGARP
XM_005039384	ADAMTS20
XM_005037072	TAF10
XM_005054309	C14H16orf71
XM_005056583	EVI2A
XM_005038551	CCDC181
XM_016298245	COL4A5
XM_005059334	LAD1
XM_016301828	LOC101813372
XM_016296212	AGAP3
XM_005051230	FETUB
XM_005043410	POLH
XM_005054364	DRC3
XM_016300815	ZWILCH
XM_005043438	WDR27

XM_005058894	S100A11
XM_005046922	C5H11orf74
XM_016306090	SLC9A2
XM_005050076	LOC101808676
XM_016300582	ATP7B
XM_005051988	TCF12
XM_016303963	LOC107604184
XM_005061593	LOC101821569
XM_016298934	ITPK1
XM_016302041	CARHSP1
XM_005049042	LOC101807582
XM_016303572	IDO2
XM_005052727	LOC101813437
XM_005047366	GPATCH2L
XM_005057073	WISP2
XM_005055863	PMP22
XM_005062304	IGSF21
XM_005050061	SLC5A9
XM_016298968	CABP4
XM_005056673	LOC101816855
XM_005056783	LOC101817428
XM_005056335	CBX2
XM_005042325	PTDSS1
XM_005055795	BARHL1
XM_005048773	HABP2
XM_016303687	SYTL1
XM_016303706	PAQR7
XM_016301660	CCDC89
XM_016305278	KIF3C
XM_005059500	PHLDA3
XM_005039461	PHLDA1

XM_016299105	GPX2
XM_005046697	GPX2
XM_005049721	DTX3L
XM_005039251	LOC101813208
XM_005049817	RNASEL
XM_005050542	GPR88
XM_005045976	NEXMIF
XM_005061804	LOC101813871
XM_005050079	MOB3C
XM_005043012	ITPKB
XM_005061100	LOC101811548
XM_005052526	SLC12A3
XM_005060823	LOC101822159
XM_005060810	DOCK8
XM_016298010	*SLC7A2*
XM_016299897	G6PC2
XM_005040638	*ZEB1*
XM_005045593	CCDC149
XM_005055395	*ALAD*
XM_005048989	*SPAG16*
XM_005060340	HAUS1
XM_005044316	SLC25A27
XM_005055265	PTPN11
XM_005056255	SLC25A10
XM_016298524	LOC101816285
XM_005061480	TSPAN9
XM_005061498	TCAF2
XM_016299390	ANXA11
XM_005059540	TAF11
XM_016304488	NCLN
XM_005051635	NR2E3

XM_005059699	P3H4
XM_005038313	*GAB2*
XM_016300131	AGL
XM_016296086	TERT
XM_016303624	FGFR1
XM_005055228	GCN1
XM_005037507	LIMS1
XM_005058597	PAFAH1B2
XM_005060625	LOC101821368
XM_005059102	UBE2Q1
XM_016297193	MZT1
XM_005038138	B3GLCT
XM_005038022	PDS5B
XM_016300038	LMO4
XM_005050724	RBP2
XM_005053530	CYFIP2
XM_005039572	STRA8
XM_005042040	*TAF4B*
XM_005042005	TUBB6
XM_005048677	SH3PXD2A
XM_005048419	*IDE*
XM_005047986	DNAJB12
XM_005038401	GSTK1
XM_005046991	DNAL1
XM_005049866	*MYOC*
XM_005050007	PLPP6
XM_005053617	NHP2
XM_005042611	LOC101815973
XM_005051099	OSTN
XM_005051315	*MECOM*
XM_005037953	CDADC1

XM_016303810	RPS25
XM_016299107	TCIRG1
XM_005039906	ACSS3
XM_016304331	MYF5
XM_005045389	ARAP2
XM_005045346	UBE2K
XM_005054795	SPECC1L
XM_005054910	MAPK1
XM_005043131	LOC101809314
XM_016297079	IMPG1
XM_005054684	TSR3
XM_005043198	LOC101822112
XM_005043614	SLC22A2
XM_005054008	RAB26
XM_005037142	SH3BGR
XM_016298043	RUNX1
XM_005037183	*RIPK4*
XM_005045614	LOC101812359
XM_005061387	NACA
XM_005046816	*CTSD*
XM_005047384	ERH
XM_005040064	LOC101810161
XM_005048086	*PAPSS2*
XM_016301575	ATP10B
XM_016300850	*SPATA5L1*
XM_016300780	AKAP13
XM_005039138	CBLL1
XM_016303057	RELN
XM_016304620	GNG10
XM_005057597	GNB1
XM_005038109	LOC101817904

XM_005053334	TRH
XM_005037520	LOC101809883
XM_005048986	ATIC
XM_005059186	KCND3
XM_005059571	LOC101810386
XM_016298945	LOC107603674
XM_016298921	LOC101813292
XM_005057359	TAF4
XM_005046501	PKP3
XM_005056669	ALDH3A2
XM_005039746	BAIAP2L2
XM_005049157	WDR12
XM_016298059	RFC1
XM_016296127	*MTBP*
XM_005045169	SPCS3
XM_005059547	*RPRML*
XM_005048151	RASGEF1A
XM_016305207	NTRK2
XM_005059489	*APOBEC2*
XM_016304871	ZCCHC7
XM_016304884	CENPK
XM_016302782	*DNAH9*
XM_005059010	*DCST2*

Supplementary Table S9. Enriched GO terms in the positive selection analysis.

# GO Accession	p-value	Odds ratio	GO term name	GO domain
GO:0005834	4.53E-12	28.86	heterotrimeric G-protein complex	cellular_component
GO:0004655	4.78E-06	60.12	porphobilinogen synthase activity	molecular_function
GO:0003924	0.001823263	2.81	GTPase activity	molecular_function
GO:0007528	6.13E-07	25.79	neuromuscular junction development	biological_process
GO:0005007	0.001399206	16.39	fibroblast growth factor-activated receptor activity	molecular_function
GO:0033754	0.001577194	60.05	indoleamine 2,3-dioxygenase activity	molecular_function
GO:0038127	0.002600032	40.03	ERBB signaling pathway	biological_process
GO:0050909	2.46E-05	17.69	sensory perception of taste	biological_process
GO:0051020	3.10E-05	16.71	GTPase binding	molecular_function
GO:0031594	1.49E-05	20.05	neuromuscular junction	cellular_component
GO:0004707	0.002100591	13.86	MAP kinase activity	molecular_function
GO:0004133	8.48E-05	60.08	glycogen debranching enzyme activity	molecular_function
GO:0004134	8.48E-05	60.08	4-alpha-glucanotransferase activity	molecular_function
GO:0004135	8.48E-05	60.08	amylo-alpha-1,6-glucosidase activity	molecular_function
GO:0005587	2.77E-07	60.15	collagen type IV trimer	cellular_component
GO:0005581	6.62E-11	17.24	collagen trimer	cellular_component
GO:0031547	0.001577194	60.05	brain-derived neurotrophic factor receptor signaling pathway	biological_process
GO:0030247	0.000343326	30.04	polysaccharide binding	molecular_function
GO:0016234	0.001112927	18.02	inclusion body	cellular_component

GO:0005605	8.48E-07	42.96	basal lamina	cellular_component
GO:0005604	2.46E-11	23.7	basement membrane	cellular_component
GO:0005978	0.000343326	30.04	glycogen biosynthetic process	biological_process
GO:0070652	0.002600032	40.03	HAUS complex	cellular_component
GO:0043121	0.001577194	60.05	neurotrophin binding	molecular_function
GO:0004364	0.000343326	30.04	glutathione transferase activity	molecular_function
GO:0006352	4.43E-06	27.34	DNA-templated transcription, initiation	biological_process
GO:0004602	0.000866659	20.03	glutathione peroxidase activity	molecular_function
GO:0005980	0.000146617	45.06	glycogen catabolic process	biological_process
GO:0005746	0.001577194	60.05	mitochondrial respiratory chain	cellular_component
GO:2001275	0.001727731	15.02	positive regulation of glucose import in response to insulin stimulus	biological_process
GO:0005201	8.50E-08	40.12	extracellular matrix structural constituent	molecular_function
GO:0006855	0.000343326	30.04	drug transmembrane transport	biological_process
GO:0009755	0.000866659	20.03	hormone-mediated signaling pathway	biological_process
GO:0015238	0.000146617	45.06	drug transmembrane transporter activity	molecular_function
GO:0007200	2.46E-05	17.69	phospholipase C-activating G-protein coupled receptor signaling pathway	biological_process
GO:0070034	0.000484473	25.75	telomerase RNA binding	molecular_function
GO:0005669	0.000807425	10.93	transcription factor TFIID complex	cellular_component
GO:0060041	1.15E-06	15.61	retina development in camera-type eye	biological_process
GO:0038063	5.02E-07	50.12	collagen-activated tyrosine kinase receptor signaling pathway	biological_process
GO:0060175	0.001577194	60.05	brain-derived neurotrophic factor-activated receptor activity	molecular_function

GO:0007064	0.001112927	18.02	mitotic sister chromatid cohesion	biological_process
GO:0001750	0.000377315	9.11	photoreceptor outer segment	cellular_component
GO:0015297	0.000144559	18.5	antiporter activity	molecular_function
GO:0003964	0.001577194	60.05	RNA-directed DNA polymerase activity	molecular_function
GO:0003721	0.001577194	60.05	telomerase RNA reverse transcriptase activity	molecular_function
GO:1903561	0.000426984	8.84	extracellular vesicle	cellular_component
GO:0005578	0.00134196	4.53	proteinaceous extracellular matrix	cellular_component

Supplementary Table S10: Summary of gene gain and loss events inferred after correcting for annotation and assembly error across all 13 species. The number of rapidly evolving families is shown in parentheses for each type of change.

	Expansions			**Contractions**			**No Change**	**Avg. Expansion**
	Families	**Genes gained**	**genes/ expansion**	**Families**	**Genes lost**	**genes/ contraction**		
Paradisaea	248 (40)	297	1.2	209 (3)	215	1.03	8555	0.009323
Astrapia	314 (40)	398	1.27	455 (31)	543	1.19	8243	-0.016537
Ficedula	329 (23)	480	1.46	560 (7)	671	1.2	8123	-0.020977
Lycocorax	513 (16)	612	1.19	338 (2)	358	1.06	8161	0.027747
Taeniopygia	1463 (17)	2009	1.37	977 (7)	1040	1.06	6572	0.091565
Ptiloris	334 (49)	401	1.2	203 (5)	219	1.08	8475	0.020200
Pteridophor	241 (13)	274	1.14	297 (6)	309	1.04	8474	-0.002997

Crow	362 (6)	480	1.33	1708 (45)	2050	1.2	6942	-0.172475

Supplementary Table S11: Assembly/Annotation error estimation and gene gain/loss rates in a single λ model in the 13 mammals included in this study compared to previous studies using fewer species.

	λ (No Error Model)	**ε (Estimated error)**	**λ (Error Model = ε)**
8 bird species in this study	0.00221	0.01025	0.00205
12 Drosophila species*	0.00121	0.04102	0.00059
10 mammal species*	0.00238	0.07324	0.00186
16 fungi species*	0.0008	0.02771	0.00061

* Dataset from Han et al. 2013 [1].

Supplementary Table S12: **Enriched GO terms in rapidly evolving birds-of-paradise families.** The number in parentheses for Rapidly evolving lineages indicates the extent of change along that lineage (ie Astrapia (+6) means that the Astrapia lineage gained 6 genes). Lineages within the BOP clade are indicated by bold text. See Figure S1 for internal node labels.

Family ID	GO accession: GO name	Rapidly evolving lineages	Enriched after FDR correction?
1	GO:0001077: transcriptional activator activity, RNA polymerase II core promoter proximal region sequence-specific binding	**Astrapia (+6)** BOP13 (-17) BOP1 (+9) Taeniopygia (+36) **Pteridophor (-4)** Crow (-12)	*
1	GO:0001078: transcriptional repressor activity, RNA polymerase II core promoter proximal region sequence-specific binding	**Astrapia (+6)** BOP13 (-17) BOP1 (+9) Taeniopygia (+36) **Pteridophor (-4)** Crow (-12)	
1	GO:0000978: RNA polymerase II core promoter proximal region sequence-specific DNA binding	**Astrapia (+6)** BOP13 (-17) BOP1 (+9) Taeniopygia (+36) **Pteridophor (-4)** Crow (-12)	*
1	GO:0000977: RNA polymerase II regulatory region sequence-specific DNA binding	**Astrapia (+6)** BOP13 (-17) BOP1 (+9) Taeniopygia (+36) **Pteridophor (-4)** Crow (-12)	*
1	GO:0001223: transcription coactivator binding	**Astrapia (+6)** BOP13 (-17) BOP1 (+9) Taeniopygia (+36) **Pteridophor (-4)** Crow (-12)	
13	GO:0004984: olfactory receptor activity	**Astrapia (+6)** **Lycocorax (-6)** Taeniopygia (+17) **BOP9 (+5)** Crow (-9)	*

26	GO:0005200: structural constituent of cytoskeleton	**BOP11 (-26)** Ficedula (+16) BOP13 (-21) BOP1 (+12) Taeniopygia (+20) **BOP9 (-3)**	*
30	GO:0001948: glycoprotein binding	**Paradisaea (+6)** **Astrapia (-3)**	
30	GO:0005041: low-density lipoprotein receptor activity	**Paradisaea (+6)** **Astrapia (-3)**	
31	GO:0001964: startle response	**Paradisaea (+3)** **BOP9 (+5)**	
31	GO:0008344: adult locomotory behavior	**Paradisaea (+3)** **BOP9 (+5)**	*
36	GO:0005112: Notch binding	**Ptiloris (+3)**	*
39	GO:0005198: structural molecule activity	**BOP9 (-3)**	*
49	GO:0003777: microtubule motor activity	**Astrapia (+3)** Crow (+15)	*
65	GO:0004222: metalloendopeptidase activity	**Astrapia (+4)** Ptiloris (-3)	*
67	GO:0005216: ion channel activity	**BOP11 (+4)** Crow (-4)	*
76	GO:0001657: ureteric bud development	**BOP11 (+3)** Crow (-4)	*
97	GO:0003958: NADPH-hemoprotein reductase activity	**Astrapia (+3)**	*
97	GO:0004517: nitric-oxide synthase activity	**Astrapia (+3)**	*
97	GO:0005272: sodium channel activity	**Astrapia (+3)**	*
102	GO:0007155: cell adhesion	**Ptiloris (-2)** Crow (+6)	*
121	GO:0060348: bone development	**Astrapia (-4)**	

121	GO:0002091: negative regulation of receptor internalization	**Astrapia (-4)**	*
130	GO:0005201: extracellular matrix structural constituent	**Paradisaea (+3)**	
138	GO:0014719: skeletal muscle satellite cell activation	**BOP5 (+1)**	*
170	GO:0006955: immune response	**Astrapia (-2)** Taeniopygia (+8) **Ptiloris (+2)** **BOP5 (-3)** Crow (-4)	*
252	GO:0019992: diacylglycerol binding	**BOP11 (+2)** **Pteridophor (+2)**	*
290	GO:0030234: enzyme regulator activity	**Paradisaea (-3)**	
312	GO:0003956: NAD(P)+-protein-arginine ADP-ribosyltransferase activity	**Paradisaea (+2)** Ficedula (+5) Taeniopygia (-3) **Ptiloris (+2)** **BOP7 (+1)** Crow (-3)	
321	GO:0017112: Rab guanyl-nucleotide exchange factor activity	**Ptiloris (-2)** **Pteridophor (+2)**	*
477	GO:0050699: WW domain binding	**BOP11 (+2)**	
584	GO:0004415: hyalurononglucosaminidase activity	**Lycocorax (+4)**	*
637	GO:0005149: interleukin-1 receptor binding	**Astrapia (+2)** **BOP9 (-2)**	*
836	GO:0017080: sodium channel regulator activity	**Paradisaea (+3)** **BOP9 (-2)**	
867	GO:0002060: purine nucleobase binding	**Paradisaea (+2)** **Ptiloris (+2)**	*
867	GO:0004645: phosphorylase activity	**Paradisaea (+2)** **Ptiloris (+2)**	*

References

1. Han, M.V., Thomas, G.W., Lugo-Martinez, J., and Hahn, M.W. (2013). Estimating gene gain and loss rates in the presence of error in genome assembly and annotation using CAFE 3. Molecular Biology and Evolution *30*, 1987-1997.